Equations of state and adsorption isotherms of low molecular non-ionic surfactants

Ivan B. Ivanov[a,*], Krassimir D. Danov[a], Dora Dimitrova[a], Maxim Boyanov[a],
Kavssery P. Ananthapadmanabhan[b], Alex Lips[b]

[a] *Laboratory of Chemical Physics & Engineering, Faculty of Chemistry, University of Sofia, Bulgaria*
[b] *Unilever Global Research Center, Trumbull, CT 06611, USA*

ARTICLE INFO

ABSTRACT

After a brief analysis of the three most widely used equations of state and adsorption isotherms, (those of van der Waals, Frumkin and Helfand–Frisch–Lebowitz with second virial coefficient) we analyze the definitions and the values of the main adsorption parameters (adsorption constant K_s, minimum area per molecule α and interaction constant β) and derive new expressions for some of them. Since it turned out that all three adsorption isotherms perform rather poorly, when used to interpret adsorption data, we applied also three more general equations—one was derived for localized adsorption long ago, but we had to derive two new equations for non-localized adsorption. We subject all 6 equations—the simple ones and the three generalized, to rigorous numerical analysis and discussion of the results. Our overall conclusion is that in some cases all equations can describe qualitatively the observed phenomena, but only the new equation of state, proposed by us for non-localized adsorption on fluid interface (and the respective adsorption isotherm), lead to correct quantitative description of the adsorption and the related parameters. In Appendix A we analyze the shortcomings and the source of errors in the fitting procedures.

1. Introduction

The non-ionic surfactants are important ingredients in many industrial products—the most trivial example are soaps, but they play important role also in many other technological and biological processes. Besides, depending on the conditions, they can acquire charge and then they become ionic/non-ionic mixtures, very complicated and difficult for analysis. On the other hand, they serve also as raw products for synthesis of important ionic surfactants and it is difficult sometimes to understand the behavior of the latter without good understanding of their non-ionic skeleton. Last, but not least, because of the low repulsion between their hydrophilic heads, the simple non-ionic surfactants had strong tendency to aggregate not only as micelles, but also to form several bulk and surface phases and various surface aggregates, which are interesting not only because they change the surface behavior but often simply from esthetic view point like in the Vollhardt articles related to chirality (see e.g. [1]). Of course, the experts in the

area are not only admiring the beautiful pictures, but are applying sophisticated experimental and theoretical tools to explain and use them. D. Vollhardt has also published numerous theories of such complicated phenomena. As examples we will cite only two subjects, to some extent related to the present article: phase transition between condensed phases of different compressibility [2] and mixed monolayers of fatty acids [3]. (An extensive review of complex phenomena, involving surfactants can be found in [4].) However, very often some theories are based on or are modifications of several simple adsorption equations, the most widely used being those of Langmuir [5] (and its modification by Frumkin [6]) and that of Volmer [7], which has been extended by adding an attractive term to become two-dimensional (2D) analog of the 3D equation of van der Waals. For reasons, which will become clear later, we will consider also another, less popular equation, that of Helfand, Frisch and Lebowitz (HFL)—in order to be able to compare it with the equations of van der Waals and Frumkin we added also an attraction term similar to that in Eq. (6), see Eq. (15) below. All these equations suppose that the adsorbed layer consists of rigid circular discs (possibly interacting through van der Waals forces) lying in a plane coinciding with or parallel to the interface, i.e. they are 2D analogs of the 3D equations of state of a fluid of spherical molecules. About the effect of the thermal motion normal to the interface see Section 3.1.

* Corresponding author. Tel.: +359 2 9625310; fax: +359 2 9625643.
 E-mail addresses: ii@lcpe.uni-sofia.bg (I.B. Ivanov), KP.Ananth@unilever.com (K.P. Ananthapadmanabhan), Alex.Lips@unilever.com (A. Lips).

Table 1
Parameters from the fit with three equations of the data for adsorption of sodium dodecyl sulfate at interfaces Air/Water and Ol/Water.

Boundary	Air/water			Oil/water			Oil/water, $\beta = 0$	
	K	α, Å^2	β	K	α, Å^2	β	K	α, Å^2
Frumkin	147	31.2	0.4	321	36.6	−1.8	186	45.2
van der Waals	137	22.9	1.2	299	26.8	−1.7	206	30.8
HFL	131	15.8	2.9	284	18.5	−1.4	237	20.3

These models have physical basis and describe and/or explain the basic features of the studied phenomena. However, they contain usually at least three free parameters and in more complicated systems it is sometimes hard to imagine from the obtained data how are the adsorption parameters related and how they depend on the other properties of the system. Another problem with the multi-parameter fits, which we will demonstrate below, is that the adsorption parameters may combine in such a way that the experimental data are fitted perfectly, but the calculated values of the parameters may change significantly, depending on the theoretical model used. We are not the only ones to point out on these problems (see e.g. [8]). In a paper, devoted to ionic surfactants [9], we analyzed some of these problems, but at that time could often find solution only to part of them. In the present paper we continue and extend our previous analysis, but deal only with non-ionic surfactants with the hope that they are simpler and easier for thorough understanding. With respect to the previous paper [9] we hope to have succeeded to find explanations of a few more unclear issues.

Our goal is not to look for explanation of complicated phenomena. We realize that when somebody is working on a complicated subject, very often it is impossible to carry out deep analysis and one is forced often to use intuition, rather than rigorous approaches. We believe however that more rigorous understanding of the simple processes and systems can help work on complicated subject at least by showing to the respective researchers which hypothesis and speculations are permissible and which ones are not. That is why we are looking mainly for qualitative physical insight on the adsorption process and the structure of the adsorbed layer. Toward this aim we selected very simple experimental systems and considerably simplified the theory in the hope that this will permit more thorough analysis of the theory and the experimental data and will shed more light on the meaning of the adsorption parameters and the factors affecting them.

To make our point, we will begin by experimental verification and comparison of the above cited equations of van der Waals, Frumkin and Helfand–Frisch–Lebowitz (HFL). We obtained at that some surprising results. Although in this article we will be dealing only with non-ionic surfactants, we will demonstrate some of them on the example of an ionic surfactant, the sodium dodecyl sulfate (SDS). The reason is that the non-ionic surfactants are soluble in oils, but the presence of the oil phase allows shedding additional light on some effects, which are also important for non-ionic surfactants. We will treat the data for SDS by using the ionic counterparts of the above equations, derived in [9]—see the respective Eqs. (2.22) and (2.23) therein. In fact the relation between the isotherms for the two types of surfactant is rather direct. The appropriate variables for the fit in the case of ionic surfactants are the adsorption Γ and $C_s^{2/3}$, where C_s is the surfactant concentration. The adsorption constant K and K_s for ionics and nonionics are related: $K \propto K_s^{1/3}$. The results for SDS are presented in Fig. 1 and Table 1 (for the interface air/water we used the results of Hines [10] and for hexadecane/water we determined experimentally the adsorption isotherm). It is noteworthy that the fits were perfect, with the exception of the Langmuir fit with $\beta = 0$, and they had regression coefficients 0.999. Nonetheless the determined adsorption parameters vary very much from model to model, but
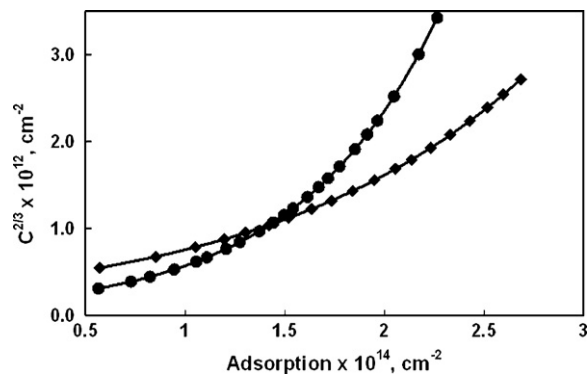

Fig. 1. Adsorption isotherms of SDS (sodium dodecyl sufate) at the interface air/water [10] (●) and hexadecane/water (◆).

systematically—for example the values of the minimum areas per molecule α are always in the order Langmuir > Volmer > HFL and those for the interaction constant β follow the opposite trend. This dependence of the parameter's values confirms our opinion in [9] that the good fit is by no means a criterion for correct results.

Another strange result is the large negative values of β for O/W, which should be in fact zero, because of the similarity between the hydrophobic surfactant tails and the oil [11]. As a matter of fact at least for HFL model we obtained for O/W perfect fits by setting $\beta = 0$ and the value of α so obtained (last column) is close to the one, which we will show in our subsequent article by using more refined equations. Another surprise was that the extended HFL equation (with account for the attraction), which we believed to be the best, gave the worst results for the interface air/water.

The overall conclusion we reached from this analysis is that the three models, presented above, lead to inconsistent results for the adsorption parameters. This confirms L. D. Landau opinion that "*The experimental data can be fitted by any not too wild theory, provided that it contains enough undetermined constants*". In order to find the reason for this we decided to analyze as thoroughly as possible both the structure of the equations and the meaning and the role of the parameters. In fact, attempt for such analysis was already done in [9], but it was not always complete. Hence, we will present briefly again part of this analysis (in some cases extended) for convenience of the reader, the more so that we will need the results for the present analysis as well. We will present also some new results, which we hope explain some of these paradoxes and help removing them.

The paper is organized as follows. In Section 2 we present and briefly analyze the equations of state and adsorption isotherms of van der Waals, Frumkin and Helfand–Frisch–Lebowitz. Since detailed analysis is impossible without deeper understanding of the theoretical expressions and the values of the main adsorption parameters (adsorption constant K_s, minimum area per molecule α and interaction constant β), Section 3 is devoted to their analysis and derivation of some new expressions for them. It turned out that the poor performance of all three adsorption isotherms, when applied to adsorption data could not be explained only by defects of the adsorption parameters. Hence, in Section 4 we decided to deal with more general equations—one was derived for localized adsorption long ago, but we had to derive two new equations for non-localized adsorption. After describing shortly the method of data processing in Section 5, in Section 6 we subject all 6 equations—the three simple and the three generalized, to rigorous numerical analysis and discussion of the results. The article terminates by conclusion and Appendix A, analyzing the shortcomings and the source of errors in the fitting procedures.

2. Simple equations of state and adsorption isotherms

We will begin by presenting and analyzing the two most widely used surface equation of state (EOS), which are often used as basis for generalizations or extensions: the equations of Frumkin and van der Waals. Since they differ only by their hard core parts, which were suggested by Langmuir and Volmer respectively, we will often call them equations (or models) of Langmuir or Volmer.

2.1. Equation of van der Waals

To make our viewpoint more clear, we will modify for a 2D-system the derivation of Landau and Lifshits (Chapter 7 in [12]) of the original 3D van der Waals equation, which is the most transparent physically. Let us take the virial expansion for the free energy F of a 2D fluid of area A consisting of N_a circular discs each of diameter d:

$$F = N_a F_0(T) + N_a kT \ln\left(\frac{N_a}{A}\right) + kT B_2 \frac{N_a^2}{A};$$

$$B_2 = \pi \int_0^\infty \left[1 - \exp\left(-\frac{u}{kT}\right)\right] r \, dr \tag{1}$$

where kT is the thermal energy, B_2 is the second virial coefficient and $u(r)$ is the interaction energy between two discs at a distance r. It is assumed further that at $r < d$ the molecules interact like rigid bodies with energy $+\infty$ and at $r > d$ the energy is small, $|u/(kT)| \ll 1$. Then

$$B_2 = \alpha_V - b; \quad \alpha_V = \frac{\pi d^2}{2} = 2\alpha; \quad b = -\frac{\pi}{kT}\int_d^\infty u(r) r \, dr \approx \frac{\alpha_V}{2}\frac{w}{kT} \tag{2}$$

where α is the true area of the disc, w is the interaction energy at contact and by α_V we have denoted the contribution to B_2 from the repulsive energy (the subscript "V" denotes that the respective values pertain to the Volmer model). If one assumes that $u < 0$ for any $r > d$, the constant b will be positive. If $u(r)$ is described by London's equation, the integral can be solved with the result shown in Eq. (2). The ratio $w/(kT)$ will be denoted hereafter by β. If the surface layer is not dense, $N_a \alpha_V / A \ll 1$, one can use the relation

$$\ln(A - N_a \alpha_V) \approx \ln A - \frac{N_a \alpha_V}{A} \tag{3}$$

to eliminate $\ln A$ from Eq. (1) and to obtain

$$F = N_a F_0(T) - N_a kT \ln\left(\frac{A - N_a \alpha_V}{N_a}\right) - kT\beta\frac{N_a^2 \alpha_V}{2A} \tag{4}$$

By using the fundamental equation for an isothermal one-component 2D system with chemical potential μ and surface pressure $\Delta\sigma$:

$$dF = -\Delta\sigma \, dA + \mu \, dN_a \tag{5}$$

one obtains with Eq. (4) the 2D equation of state (EOS):

$$\frac{\Delta\sigma}{kT} = \frac{\Gamma}{1 - \alpha_V \Gamma} - \frac{\alpha_V \beta}{2}\Gamma^2 \tag{6}$$

where $\Gamma = N_a/A$ is the adsorption.

The above derivation shows the limitations of the van der Waals EOS: it is valid only for small interaction energy (small β) and low surface coverage $\alpha_V \Gamma \ll 1$, when only double collisions play a role (only B_2 was accounted for). Landau and Lifshits [12] warned that "*the constant b (in the 3D van der Waals equation) can by no means be regarded as fourfold "volume of the molecule" even for one-molecular gas*". Similar conclusion should be true of course for the constant α_V in the 2D van der Waals equation, Eq. (6).

The adsorption isotherm can be obtained by integrating Gibbs equation, which for isothermal one-component adsorbed layer with surfactant bulk concentration (or activity) C_s reads:

$$d(\Delta\sigma) = kT\Gamma \, d(\ln C_s) \tag{7}$$

By substituting here $\Delta\sigma$ from Eq. (6) and integrating one finds:

$$K_s C_s = \frac{\Gamma}{1 - \alpha_V \Gamma} \exp\left(\frac{\alpha_V \Gamma}{1 - \alpha_V \Gamma} - \beta\alpha_V \Gamma\right) \tag{8}$$

where

$$K_s = \delta_s \exp\left(\frac{E_A}{kT}\right) \tag{9}$$

is the adsorption constant, E_A is the free adsorption energy (i.e. the free energy for bringing the surfactant molecule from the bulk solution into the adsorbed layer) and δ_s has the meaning of "*thickness of the adsorbed layer*". These quantities are discussed later.

Another useful equation is related to the Gibbs elasticity, E_G, which is defined as

$$E_G = \frac{d(\Delta\sigma)}{d \ln\Gamma} \tag{10}$$

In dimensionless form, with $\theta = \alpha_V \Gamma$, Eqs. (6) and (10) yield

$$\frac{\alpha_V E_G}{kT} = \frac{\theta}{(1 - \theta)^2} - \beta\theta^2 \tag{11}$$

There are several experimental methods for measurement of E_G, providing possibility for additional checking the adsorption model and parameters but this is beyond the scope of this study.

2.2. Equation of Frumkin

It is based on the Langmuir EOS. The latter is a rigorous equation for adsorption on a 2D lattice of adsorption centers if the following conditions hold [13]: (i) each center can be occupied only by one molecule; (ii) the adsorbed molecules cannot interact with each other neither by attractive nor by repulsive forces – this means that the area occupied by the adsorbed molecule must be equal or smaller than the area pertaining to the center; (iii) the combinatorial formula the derivation is based upon describes the distribution of N_a undistinguishable molecules over M numbered centers – this means that the molecules cannot exchange positions over the surface and jump from center to center even if there are non-occupied centers. The combination of these conditions cannot be realized with a fluid adsorbed layer. Belton and Evans [14] succeeded to derive Langmuir EOS for liquid mixtures but only on the condition that the solvent and the solute have exactly the same size—in this case removing one solvent molecule from the interface in fact creates a center for adsorption of a solute molecule and *vice versa*. They showed that small difference in sizes leads to considerable errors.

Nonetheless from its very derivation the EOS of Langmuir has been widely applied to adsorbed fluid layers. One possible reason is the fact that its integration by means of Gibbs adsorption isotherm to eliminate Γ leads exactly to the empirical Szyszkowski equation, which was shown to describe well the dependence of the surface tension σ on the surfactant concentration C_s for low molecular surfactants. This is not so surprising since the size of the hydrophilic groups of these substances is not much different from that of water.

However, attempts to treat the adsorption of other molecules by using Langmuir equation failed. Frumkin [6] attributed it to the intermolecular interaction and suggested, by analogy with van der Waals equation of fluids, to add a term accounting for this effect through β (the first term in the right is Langmuir's equation):

$$\frac{\Delta\sigma}{kT} = -\frac{1}{\alpha_L} \ln(1 - \alpha_L \Gamma) - \alpha_L \beta\Gamma^2; \quad \beta = \frac{w_L}{kT} \tag{12}$$
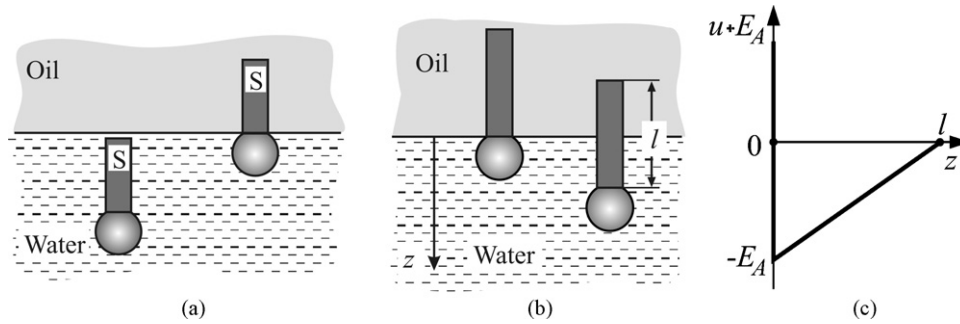
Fig. 2. Schematic presentation of the process of adsorption and the related energy u. (a) Molecules in the water phase and in adsorbed state. (b) Adsorbed and partially immersed molecule. (c) Energy u of a molecule immersed at a distance z from the interface.

In fact, the equation of Frumkin is analogous to the equation of Bragg and Williams [see e.g. reference [13], Chapter 14], who introduced in the model of Langmuir interaction between closest neighbors. Their equation differs from that of Frumkin only by the attractive term which they found to be $z_n \alpha_L \beta \Gamma^2 / 2$, where z_n is the number of closest neighbors (usually 4 or 6) and w_L in β is replaced by the interaction energy w_1 *with one neighbor only*. Frumkin equation is obtained by setting $z_n = 2$, which corresponds to adsorption on a line. However, Frumkin equation does not coincide with the exact EOS for adsorption on a line (see Eq. 14.16 in [13]).

The respective adsorption isotherm is obtained again by integrating Gibbs equation along with the EOS:

$$K_s C_s = \frac{\Gamma}{1 - \alpha_L \Gamma} \exp(-2\beta \alpha_L \Gamma) \tag{13}$$

and the relation for the Gibbs elasticity is (with $\theta = \alpha_L \Gamma$)

$$\frac{\alpha_L E_G}{kT} = \frac{\theta}{1 - \theta} - 2\beta \theta^2 \tag{14}$$

2.3. Equation of Helfand–Frisch–Lebowitz (HFL)

Reiss et al. [15] developed a very astute procedure, (which they called "*Scaled Particle Theory*") for treating systems of hard core particles. Unfortunately nobody has succeeded to apply it to particles with attraction. They solved exactly several problems, related to hard particles, but it turned out that the 2D case (hard discs at interfaces) has in principle no exact solution. Nevertheless, Helfand et al. [16] succeeded to derive an almost exact simple 2D EOS. It is impossible to present in a concise manner their theory and we refer the interested reader to the original paper. In order to be able to compare the theory with the equations of van der Waals and Frumkin we added to their (hard core) result an attraction term as in Eq. (6) but in order to keep the definition of $\beta = w/(kT)$ unchanged, we substituted there 2α for α_V, see Eq. (2). Thus the *modified* HFL equation became:

$$\frac{\Delta \sigma}{kT} = \frac{\Gamma}{(1 - \alpha \Gamma)^2} - \alpha \beta \Gamma^2 \tag{15}$$

The respective adsorption isotherm is:

$$K_s C_s = \frac{\Gamma}{1 - \alpha \Gamma} \exp\left[\frac{\alpha \Gamma(3 - 2\alpha \Gamma)}{(1 - \alpha \Gamma)^2} - 2\beta \alpha \Gamma \right] \tag{16}$$

and the Gibbs elasticity (with $\theta = \alpha \Gamma$)

$$\frac{\alpha E_G}{kT} = \frac{\theta(1 + \theta)}{(1 - \theta)^3} - 2\beta \theta^2 \tag{17}$$

3. Analysis of the adsorption parameters

3.1. Adsorption constant and thickness of the adsorbed layer

According to Eq. (9) the adsorption energy, E_A, is the major factor determining the value of the adsorption constant, K_s. It can be calculated by finding the change in free energy involved in the transfer of a molecule from the water phase to the upper hydrophobic phase (oil, in Fig. 2). We will consider a surfactant with a paraffinic chain with n_c carbon atoms, length per –CH$_2$– group $l_1 \approx 0.126$ nm, cross-sectional area $\alpha_c \approx 0.20$ nm^2, and lateral area (along the chain) pertaining to one –CH$_2$– group $\alpha_l \approx 0.21$ nm^2 (all data are based on the geometrical parameters of the paraffinic chain as determined by Tanford [17]). Let w_c be the energy of transfer of one –CH$_2$– group. The energy of transfer of the top –CH$_3$ group, is larger than w_c because of its larger area, but since there are no precise data for this energy for the interface air/water we will account for this approximately by adding an additional term w_c as for one more methyl group.

An effect, usually neglected (and we added it), is the displacement of an area α_c from the interface when the surfactant tail is adsorbed. The polar head remains immersed in the water phase and it should not contribute much to the adsorption energy when only short range interactions are effective. The situation could be different with the electrostatic interaction of the head with the interface for ionic surfactants or if there is change of hydration of the polar head. Hence, we will add a term E_h to account for this effect.

On the other side, one must account also for the partial immersion of the hydrophobic chain, due to the fact that the adsorption energy of a –CH$_2$– unit is of the order of kT. If one assumes that the surfactant molecules is perpendicular to the interface as shown in Fig. 2b, its energy $u(z)$ will vary with the immersion depth as depicted in Fig. 2c and can be written as

$$u = -E_A + w_l z \tag{18}$$

where w_l is the immersion energy per unit length and E_A is the adsorption energy. Then the average immersion depth z_{imm} of the aliphatic chain will be:

$$z_{imm} = \int_0^l \exp(-bz) \, dz \approx \frac{1}{b} = \frac{kT}{w_c} l_1 \tag{19}$$

where $b = w_l/(kT) = w_c/(kTl_1)$. And since $kT \approx w_c$, one must conclude that $z_{imm} \approx l_1$, i.e. that the first –CH$_2$– group will be entirely in the water phase and its contribution to the adsorption energy E_A will be negligible. This effect will cancel the additional contribution of the terminal –CH$_3$ group, which was assumed above equal to w_c.

Thus, the overall balance of energy leads to:

$$E_A = E_h + w_c n_c + \sigma_{OW} \alpha_c = E_0 + w_c n_c \tag{20}$$

where $E_0 \equiv E_h + \sigma_{OW}\alpha_c$ is that part of the adsorption energy, which is independent of the chain length. Equation similar to the second Eq. (20) was postulated by Davies and Rideal [19] based on experimental data. However, unlike us, they ascribed E_0 only to the adsorption energy of the polar head.

The result, Eq. (20), was used by us to derive an explicit equation for the "thickness of the adsorbed layer" [9] and the adsorption constant K_s. From Eq. (18), Boltzmann equation and Gibbs definition of Γ one can write:

$$\Gamma = \int_0^l [C_s(z) - C_s]\,\mathrm{d}z \approx \frac{kT}{w_l}\exp\left(\frac{E_A}{kT}\right)C_s = K_sC_s \qquad (21)$$

The comparison with Eq. (9) shows that $\delta_s = kT/w_l$. For air/water interface $\delta_s = 1.16\,\text{Å}$ [9]. This result will be checked below. The effect of the term $\sigma_{OW}\alpha_c$ will be checked separately in a subsequent paper by using adsorption data obtained with several oil phases with different interfacial tension.

When deriving Eqs. (19) and (21) it was tacitly assumed that all surfactant molecules are fluctuating synchronically, that is they all remain in the same plane which is moving up and down. In reality, their motion is not coordinated so that the collision between the molecules might occur when the immersion of the colliding molecules is different which should affect the minimum area α. This effect was investigated in [18], where a general theory was developed and it was shown that in most cases it is small. The situation might be different if the transfer energy w_l is small, which will be so if there are double bonds close to the hydrophilic head.

3.2. Minimum (proper) area of a molecule α

We used a simple method to find the dependence of α on Γ for Langmuir and Volmer equations, based on the fact, that α in the HFL equation of state, Eq. (15), is the true area per molecule $\alpha = \pi d^2/4$. To avoid confusion we will denote here the latter by α_H and $\alpha_H\Gamma_H$ by θ_H, and will use the notations θ_L and α_L, θ_V and α_V for the equations of state of Langmuir and Volmer, respectively. All three EOS (with $\beta = 0$) can be written as [see Eqs. (6), (12) and (15)]:

$$\frac{\Delta\sigma}{kT\Gamma} = f_M(\theta_M) \qquad (22)$$

where f_M is a function of θ_M different for the models of Langmuir, Volmer or HFL (hence the subscript M, indicating that the function is model dependent). Since the left hand sides of these equations do not depend on the model, the right hand sides must be equal. This leads to the equations:

$$-\frac{1}{\theta_L}\ln(1 - \theta_L) = \frac{1}{1 - \theta_V} = \frac{1}{(1 - \theta_H)^2} \qquad (23)$$

For small θ one can expand the above expressions in series and by keeping only the linear terms in the expansions one finds

$$\alpha_L = 2\alpha_V = 4\alpha_H; \quad \text{at } \theta \to 0 \qquad (24)$$

The second equation in Eq. (23) can be solved easily and leads to the exact relationship for the Volmer model:

$$\frac{\alpha_V}{\alpha_H} = 2 - \theta_H \qquad (25)$$

The exact relation between θ_L and θ_H from Eq. (23) can be found only numerically and the obtained dependence of α_L/α_H vs. θ_H is shown in Fig. 3. Its asymptotic behavior at $\theta_H \to 0$ or $\theta_H \to 1$ is respectively

$$\frac{\alpha_L}{\alpha_H} = 4 - \frac{14}{3}\theta_H \quad \text{at } \theta_H \to 0 \quad \text{and} \quad \frac{\alpha_L}{\alpha_H} = 2 - \theta_H \quad \text{at } \theta_H \to 1 \qquad (26)$$

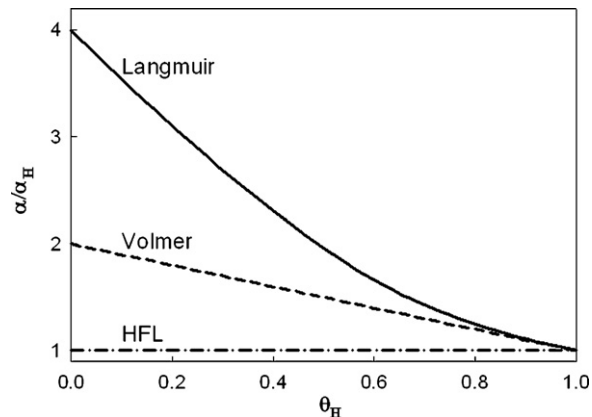**Fig. 3.** Theoretical dependence of the minimum area per molecule α/α_H (relative to the value α_H of the isotherm HFL) for three models as a function of the degree of surface coverage $\theta_H = \alpha_H\Gamma$.

The second equation coincides with Eq. (25). This fact explains why the exact solutions for α_V/α_H and α_L/α_H in Fig. 3 merge already around $\theta_H = 0.7$–0.8.

Russanov [20] had ideas similar to ours about the dependence of the minimum area per molecule α on the adsorption Γ. By using a different approach from ours he also found for Langmuir model the limiting values 4 and 1 at $\theta_H \to 0$ and $\theta_H \to 1$, respectively. For the initial slope at $\theta_H \to 0$ he obtained however -6.616 instead of our value $-14/3$, see Eq. (26).

To check the reliability and applicability of the results for α for the three models we performed numerical comparison between the results they lead to. The hard core part of HFL equation has been checked numerically by Monte Carlo and dynamical calculations (see Fig. 4, adapted by us from [16] by adding the data for Volmer and Langmuir models) and showed excellent agreement with these data almost up to complete coverage. At the same figure are plotted the data, obtained from the models of Langmuir and Volmer [the hard core parts of Eqs. (6) and (12), respectively]—the differences are obvious.
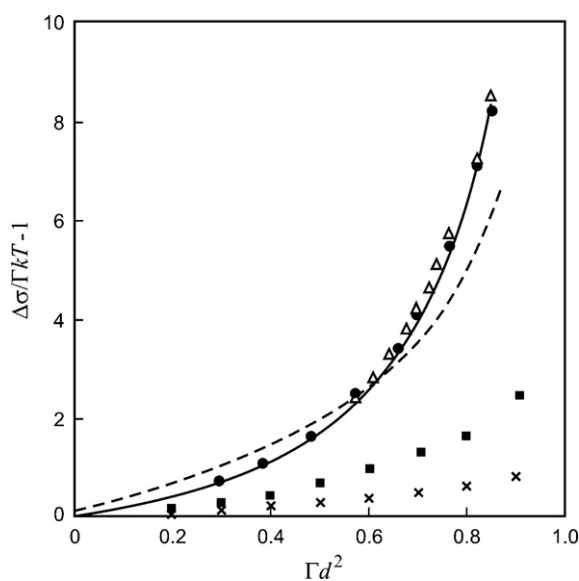

Fig. 4. Comparison of the hard core parts of three two-dimensional equations of state: solid line-Eq. (15) of HFL; ●: Monte Carlo calculations of Wood; △: dynamical calculations of Alder and Wainwright; – – – –: Lennard–Jones–Devonshire cell theory; ■: Volmer Eq. (6); ×: Langmuir Eq. (12).

Such differences are revealed also by the virial expansions of the hard core parts of the three equations. The expansion of the hard core part of the HFL Eq. (15) is:

$$\frac{\Delta\sigma}{kT\Gamma} = 1 + 2\theta + 3\theta^2 + 4\theta^3 + 5\theta^4 + \cdots \tag{27}$$

to be compared with the exact result [16]:

$$\frac{\Delta\sigma}{kT\Gamma} = 1 + 2\theta + 3.128\theta^2 + 4.262\theta^3 + 4.95\theta^4 + \cdots \tag{28}$$

The respective expansions for Langmuir and Volmer models are:

$$\frac{\Delta\sigma}{kT\Gamma} = 1 + \frac{\theta}{2} + \frac{\theta^2}{3} + \frac{\theta^3}{4} + \frac{\theta^4}{5} + \cdots \tag{29}$$

$$\frac{\Delta\sigma}{kT\Gamma} = 1 + \theta + \theta^2 + \theta^3 + \theta^4 + \cdots \tag{30}$$

The large discrepancy with the exact result for HFL should not be surprising for the model of Langmuir, which was developed for a very different (localized) monolayer, but the Volmer model is supposed to work just as HFL model for a fluid monolayer. The results from this section lead to the important conclusion that the area per molecule, determined by using a model isotherm (not based on HFL), may not be a true physical constant, but may depend on the model used and the adsorption, Γ. The other, even more important, conclusion is that it is not enough to use the correct hard core part (that of HFL) to obtain correct EOS. Indeed, the results shown in Table 1, obtained by the modified HFL Eq. (15), are by no means better than the ones obtained by Frumkin and van der Waals equations. On the other hand, when the same data are treated for O/W by setting $\beta = 0$, the result for HFL is quite reasonable. This shows that the blame must be put also on β and one must find a more correct way to account for the intermolecular interaction.

As already pointed out all three considered models are based on the assumption that the surfactant molecules are hard interacting discs, analogously to most of the bulk model EOS, where the molecules are considered as hard interacting spheres. We accounted in part for the role of the surfactant tails (which we considered as solid rods) in the adsorption constant, K_s, both by the adsorption energy and the immersion of the tails, determining the thickness of the adsorbed layer δ_s. However, the tails are by no means rigid rods, because even simple tails, like the aliphatic chains, can perform (hindered) rotation around the C–C bonds and can therefore change conformation. As a result if the chain is long enough it will behave like a polymer and form coils, which might be larger than the hydrophilic group and will determine the minimum area per molecule, α. The shorter chains may remain approximately linear, but have the freedom to be inclined or even to lye flat on the interface. Which one of these possibilities will take place depends on the relative contribution of the respective process to the free energy of the system. Many researchers account in one way or another for some of these complications in order to explain some experimental observations. However, we formulated as our goal the understanding of the very basic effects and dealing with these complications is beyond the scope of this article, the more so that their rigorous treatment usually requires special techniques—the interested reader can find detailed discussion of some of these effects in ref. [4]. We will return to the discussion of the simplest case—rigid rods perpendicular to the interface later, in Sections 3.3 and 6.

3.3. The interaction constant, β

This is the most controversial and the most difficult for determination constant. The error of its determination is very rarely as small as 10%. It is usually 20–25% but can be even higher than 100% (for more detailed discussion see Appendix A). That is why we decided to derive an approximate expression for β just to have some benchmark for comparison of the results of the different fits.

In fact constant β is part of the second virial coefficients B_2 and enters in it always as a product with α, see Eqs. (6), (12) and (15).

The interaction part of the second virial coefficient, B_2, is defined as [13]

$$B_{2,\text{int}} = \pi \int_d^\infty \left[1 - \exp\left(-\frac{u_{\text{int}}}{kT} \right) r \, dr \right] \tag{31}$$

where u_{int} is the interaction energy between two surfactant molecules, r is the separation between them and $d = (4\alpha/\pi)^{1/2}$ is the closest distance. We will suppose that the molecules are perpendicular to the interface. The integral accounts for the contribution from the long range (usually attractive) interactions.

We will assume that $|u_{\text{int}}| \ll kT$ so that the integrand in the right-hand side of Eq. (31) can be expanded in series with respect to $u_{\text{int}}/(kT)$. The most common case is the attractive London interaction. In this case one can model the tails of the surfactant molecules as a line with uniform linear molecular density, $\rho_t = 1/l_1$ each with constant of interaction with another $-CH_2-$ group $L = 3\alpha_p I_0/4$ where α_p is polarizability and I_0 is the ionization potential [11]. In this case the interaction energy is calculated as

$$u_{\text{int}}(r) = -\rho_t^2 L \int_0^l \int_0^l [r^2 + (z_2 - z_1)^2]^{-3} \, dz_1 \, dz_2 \tag{32}$$

where z_1 and z_2 are the vertical coordinates of the interacting $-CH_2-$ groups.

Performing the integration of Eq. (32), substituting the result in Eq. (31) and having in mind Eq. (15) one finds:

$$B_{2,\text{int}} = -\frac{\pi\rho_t^2 L}{4d^2 kT} \frac{l}{d} \arctan\left(\frac{l}{d} \right) = -\alpha\beta \tag{33}$$

Therefore, one can use the second virial coefficient for the calculation of β if α is known. In the case $l \gg d$ one can write:

$$B_{2,\text{int}} = -\frac{\pi\rho_t^2 L}{4d^2 kT} \left[\frac{\pi}{2}\frac{l}{d} - 1 + \frac{1}{3}\left(\frac{d}{l}\right)^2 - \frac{1}{5}\left(\frac{d}{l}\right)^4 + \cdots \right] \tag{34}$$

Then one can use the following asymptotic expression for estimation of β:

$$B_{2,\text{int}} \approx -\frac{\pi^2\rho_t^2 Ll}{8d^3 kT} = -\alpha\beta \tag{35}$$

4. Generalized equations for interacting surfactants

4.1. Localized adsorption (Langmuir model)

We will try now to use more general analogs of the equations of Frumkin, Eq. (12), van der Waals, Eq. (6), and the extended equation of HFL, Eq. (15), by accounting more correctly for the effect of the intermolecular interaction. We will begin by Langmuir model, since a generalized equation, much more precise than Fumkin equation, is known. It was derived first by Bethe and later by Guggenheim (see [13], Chapter 14) who called it *quasi-chemical approximation*. The reason for this title is that the basic equation is in fact the equilibrium constant between the pairs 0–0, 0–1 and 1–1 (0 stands for an empty and 1 stands for an occupied center) with free energy w. The resulting EOS is (see also [9]):

$$\frac{\alpha_L \, \Delta\sigma}{kT} = -\ln(1-\theta) - \frac{z_n}{2}\ln\left[\frac{\beta_n + 1 - 2\theta}{(\beta_n + 1)(1-\theta)} \right];$$
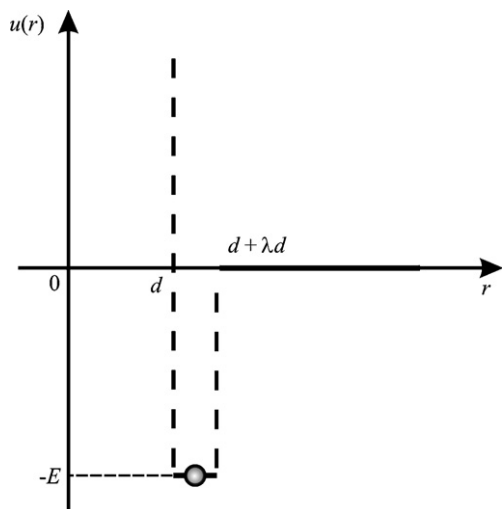
$$\beta_n \equiv [1 + 4\beta\theta(1-\theta)]^{1/2} \tag{36}$$

Fig. 5. Sketch of "sticky potential" of width λd and depth E for a molecule of length (or diameter) d.

The adsorption isotherm is

$$K_s C_s = \frac{\Gamma}{1-\theta} \left[\frac{1}{1+\beta} \frac{1+\beta_n+2\beta(1-\theta)}{1+\beta_n+2\beta\theta} \right]^{z_n/2} \tag{37}$$

and the Gibbs elasticity:

$$\frac{\alpha_L E_G}{kT} = \frac{\theta}{1-\theta} - \frac{2z_n\beta\theta^2}{\beta_n(\beta_n+1)} \tag{38}$$

In order to compare Eqs. (36) and (12), we expanded the interaction term, that is the second term in the right-hand side in Eq. (36), in series:

$$\frac{\alpha_L \Delta\sigma}{kT} = -\ln(1-\theta) - \frac{z_n\beta}{2}\theta^2 + z_n\beta^2\theta^3 - \frac{3+10\beta}{4}z_n\beta^2\theta^4 + \cdots \tag{39}$$

This result suggests three important conclusions: (i) the hard core part of the Langmuir equation (the first term in the right) is correct; (ii) the Frumkin equation, Eq. (12), accounts accurately for the interaction up to the second virial coefficient (the term with θ^2); (iii) more importantly, only in the second virial coefficient the interaction contribution is proportional to β, whereas in the third virial coefficient it is proportional to β^2, and so on. This means that if $\beta \ll 1$, it is legitimate even for large θ to keep only the term with the second virial coefficient (proportional to β) from the interaction contributions. Hence, the Langmuir–Frumkin equation is exact if $\beta \ll 1$, *provided that the adsorption is really localized*.

4.2. Non-localized 1D adsorption (Volmer model)

This problem can be solved exactly if one uses the approach of the "sticky potential" developed by Baxter [21]. It is based on the fact that in many cases the width of the interaction well is very small and the attraction between the particles becomes sizable only when they almost touch each other. The assumed potential distribution is sketched in Fig. 5 by dashed line. Up to the minimum distance d between the particles the potential energy u is $+\infty$, then in the potential well between d and $d+\lambda d$ it remains constant and equal to $-E$, after which it becomes zero. When the particles are approaching each other, $\lambda \to 0$, but $E \to -\infty$ in such a way that the product λE remains equal to the interaction energy at contact w. Briefly, this means that the interaction energy is represented by a δ-function of Dirac.
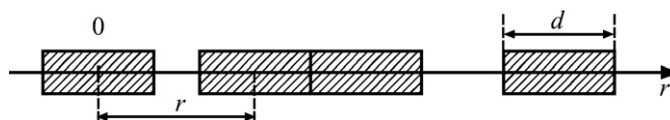

Fig. 6. Scheme of one-dimensional adsorption: sticks of zero thickness and length d strung on a thread.

The system we will consider (see Fig. 6) represents a set of N_a sticks each of length d strung on a thread of total length L_1 which is analog for this case to the area A of 2D systems. The moving particles in direction r exert a 1D pressure $\Delta\sigma$.

The convenient thermodynamic potential for this problem is the isothermic-isobaric potential $N_a\mu$ ([13], Chapter 1):

$$N_a\mu = F + L_1\,\Delta\sigma; \quad d(N_a\mu) = L_1\,d(\Delta\sigma) + \mu\,dN_a \tag{40}$$

with partition function Δ_p:

$$N_a\mu = -kT\,\ln\Delta_p \tag{41}$$

$$\Delta_p = \int_0^\infty Z \exp\left(-\frac{L_1\,\Delta\sigma}{kT}\right) d\left(\frac{L_1\,\Delta\sigma}{kT}\right); \quad Z = Z_{hc}\exp\left(-\frac{u}{kT}\right) \tag{42}$$

where Z is the configurational integral. Its hard core part Z_{hc} can be found by substituting the first term in the right-hand side of Eq. (6) in Eq. (5) (both written for one dimension with N_a = constant) and integrating. The result is:

$$F_{hc} = -kT\,\ln Z_{hc} = -kT\ln(L_1 - N_a d) \tag{43}$$

The adsorption isotherm is obtained from the second Eq. (40) along with Eq. (41):

$$\frac{1}{\Gamma} = -\frac{kT}{N_a}\left[\frac{\partial\,\ln\Delta_p}{\partial(\Delta\sigma)}\right]\Bigg|_{N_a}; \quad \Gamma \equiv \frac{N_a}{L_1} \tag{44}$$

By introducing the dimensionless variables

$$x \equiv r\frac{N_a\,\Delta\sigma}{kT}; \quad x_0 \equiv d\frac{N_a\,\Delta\sigma}{kT} \tag{45}$$

we can put Eq. (42) in a simpler form:

$$\Delta_p = \frac{kT}{\Delta\sigma}\int_{x_0}^\infty (x - x_0) \exp\left[-x - \frac{u(x)}{kT}\right] dx \tag{46}$$

The integral splits into two parts, which are easily solvable: (i) $x_0 < x < (1+\lambda)x_0$, where u is constant ($u = -E$) and (ii) $(1+\lambda)x_0 < x < \infty$ where $u = 0$. In the result one must use the sticky approximation, which means to set $\exp[E/(kT)] = w/(\lambda kT) = \beta/\lambda$. Upon inserting the result in Eq. (46) and expanding the appearing exponential function of $\lambda \to 0$ in series up to the linear term, one obtains a quadratic equation with respect of $\Delta\sigma/(kT\Gamma)$, whose solution is the sought for 1D EOS[1]:

$$\frac{\Delta\sigma}{kT} = \frac{\Gamma}{2\alpha\beta}\left[-1 + \left(1 + 4\beta\frac{\alpha\Gamma}{1-\alpha\Gamma}\right)^{1/2}\right] \tag{47}$$

where $\alpha \equiv d$. This result can be rationalized to acquire more convenient and transparent form:

$$\frac{\Delta\sigma}{kT} = \frac{\Gamma}{1-\alpha\Gamma}\frac{2}{1+R_\beta^1}; \quad R_\beta^1 \equiv \left(1 + 4\beta\frac{\alpha\Gamma}{1-\alpha\Gamma}\right)^{1/2}; \quad \beta = \frac{w}{kT} \tag{48}$$

---

[1] This result was first obtained in [22] by using a somewhat different approach.
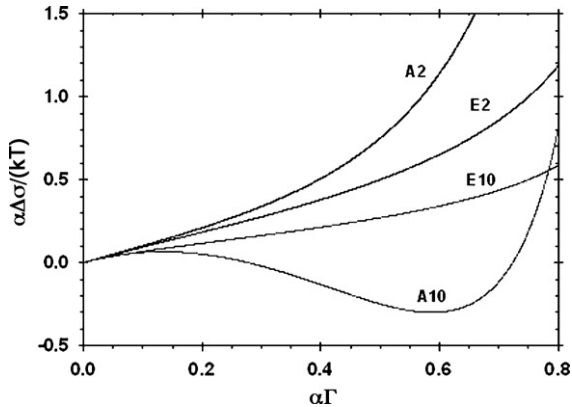
Fig. 7. Comparison of the exact *E* (Eq. (48)) and approximate *A* (Eq. (6)) equations of Volmer. The numbers indicate the values of $\beta = 2$ and $\beta = 10$, respectively.

In view of further discussions we will expand the result in series with respect to β:

$$\frac{\Delta\sigma}{kT} = \frac{\Gamma}{1-\alpha\Gamma}\frac{2}{1+R_\beta^1} \approx \frac{\Gamma}{1-\alpha\Gamma}$$
$$\times \left[1 - \beta\frac{\alpha\Gamma}{1-\alpha\Gamma} + 2\beta^2(\frac{\alpha\Gamma}{1-\alpha\Gamma})^2 - \cdots\right] \qquad (49)$$

The respective adsorption isotherm is obtained as usual by integrating Gibbs equation along with Eq. (48):

$$K_s C_s = \frac{\Gamma}{1-\theta}\left(\frac{2}{1+R_\beta^1}\right)^2 \exp\left[\frac{2\theta}{(1+R_\beta^1)(1-\theta)}\right] \qquad (50)$$

Some obvious conclusions follow from this result: (i) the comparison with Eq. (6) (with $\beta = 0$) reveals that Volmer equation for hard particles is rigorous only in one dimension; (ii) the van der Waals term $\alpha\beta\Gamma^2$ is obtained if in Eq. (49) one sets β^2, β^3 etc. equal to zero and if in the denominator of the term, linear in β, one neglects $\alpha\Gamma$—but then, why should one keep $\alpha\Gamma$ in the main term, multiplying the square brackets? The expansion in series of the attractive terms leads to the same conclusion:

$$\frac{\Delta\sigma}{kT} = \frac{\Gamma}{1-\alpha\Gamma}\frac{2}{1+R_\beta^1} \approx \frac{\Gamma}{1-\alpha\Gamma}$$
$$\times \left[1 - \beta\theta - (\beta - 2\beta^2)\theta^2 - (\beta - 4\beta^2 + 5\beta^3)\theta^3 + \cdots\right] \qquad (51)$$

One sees that unlike the case of localized adsorption, see Eq. (39), all virial coefficients contain terms linear in β, so that it is not obvious if one can keep only the term $\beta\theta$ as it is done in van der Waals equation, Eq. (6).

In Fig. 7 we carried out numerical comparison for two values of β of van der Waals equation, Eq. (6), and the exact Eq. (48). One sees that for small values of $\beta = 2$ and θ the van der Waals equation is reasonably close to the exact solution. They diverge however strongly for large $\beta = 10$ even when θ is small. Worst of all, at large values of β van der Waals equation exhibits phase transition, although phase transitions in one-dimensional systems are forbidden [12].

4.3. Non-localized 2D adsorption (HFL model)

It has been rigorously shown [21] that exact solution for the 2D case is impossible even for hard particles. The exact solution with sticky potential of Baxter is difficult even in the 3D case and the result is very complicated and not very convenient for use. That is why we decided to use a heuristic approach in the hope that it will

lead to an EOS more rigorous than the equations for non-localized adsorption presented in Section 2.

The starting point for us was a procedure developed by Hemmer and Stell [23] for deriving equations for 3D systems, which are exact up to terms linear in β. We modified their basic equation to make it applicable to 2D systems:

$$\Delta\sigma = (\Delta\sigma)_{hc} - \left(\frac{B}{B_{hc}} - 1\right)\left[(\Delta\sigma)_{hc} - \theta\frac{\partial(\Delta\sigma)_{hc}}{\partial\theta}\right] \qquad (52)$$

where the subscript "hc" denotes "hard core" both for the second virial coefficient B and the surface pressure ($(\Delta\sigma)_{hc} = (kT/\alpha)\theta/(1-\theta)^2$, see Eq. (15). For hard discs $B/B_{hc} - 1 = -\beta$. By inserting this and the expression for $(\Delta\sigma)_{hc}$ in the right-hand side of Eq. (52), we obtain a more general form of the HFL equation:

$$\frac{\Delta\sigma}{kT} = \frac{\Gamma}{(1-\alpha\Gamma)^2}\left(1 - 4\beta\frac{\alpha\Gamma}{1-\alpha\Gamma}\right) \qquad (53)$$

A comparison with Eq. (49) reveals that the two equations have the same structure: the respective hard core factor is multiplied by expressions differing only by the numerical coefficient. It is not difficult to realize that if instead of Eq. (48) one uses

$$\frac{\Delta\sigma}{kT} = \frac{\Gamma}{(1-\alpha\Gamma)^2}\frac{2}{1+R_\beta}; \quad R_\beta^1 \equiv \left(1 + 16\beta\frac{\alpha\Gamma}{1-\alpha\Gamma}\right)^{1/2} \qquad (54)$$

we will obtain an expansion in series of β which is identical to Eq. (53) up to the linear term in β and looks like Eq. (49) (with different numerical coefficients):

$$\frac{\Delta\sigma}{kT} \approx \frac{\Gamma}{(1-\alpha\Gamma)^2}\left[1 - 4\beta\frac{\alpha\Gamma}{1-\alpha\Gamma} + 32\beta^2(\frac{\alpha\Gamma}{1-\alpha\Gamma})^2 - \cdots\right] \qquad (55)$$

The adsorption isotherm, following from Eq. (54), is:

$$K_s C_s = \frac{\Gamma}{1-\theta}\left(\frac{2}{1+R_\beta}\right)^{((1+8\beta)/4\beta)} \exp\left[\frac{2\theta(4-3\theta)}{(1+R_\beta)(1-\theta)^2}\right] \qquad (56)$$

and the Gibbs elasticity:

$$\frac{\alpha E_G}{kT} = \frac{\theta}{(1+R_\beta)(1-\theta)^3}\left(1 + 2\theta + \frac{1}{R_\beta}\right) \qquad (57)$$

We tried to check at least approximately the reliability of Eq. (55) by two methods: (i) calculation of the third virial coefficient B_3 by the method of Kihara [24] and (ii) by solving Kirkwood integral equation (see e.g. [25]). Both methods involve very complicated and lengthy calculations, which will be published in a separate paper. Here we will give only an idea how they were done and will present the final results.

The virial expansion is

$$\frac{\Delta\sigma}{kT\Gamma} = 1 + B_2\Gamma + B_3\Gamma^2 + B_4\Gamma^3 + \cdots \qquad (58)$$

The method of Kihara for B_3 for spheres represent integration over the overlapping volumes of three spheres weighted by the respective energies of interaction, represented by square well. We modified it for three discs on a surface and applied to the final results the sticky approximation instead of square well. The expansion of Eq. (54) in terms of Γ gives $B_3 = 3\alpha^2(1 - 4\beta + 3\beta^2)$ and the obtained theoretical value by the method of Kihara was $B_3 = 3\alpha^2(1 - 4\beta + 1.33\beta^2 - 0.62\beta^3)$. Therefore, Eq. (54) gives for B_3 exactly the linear term in β, reasonably well β^2, but β^3 comes only from the next term of the expansion. These differences will be important at rather large values of β and θ, but as we will see later such values are rarely encountered with most simple surfactants. Besides, Kihara himself pointed out that the third virial coefficient is very sensitive to the shape of the potential, so that one can hardly

expect exact results from approximate potentials like "square well" or "sticky potential".

The 2D analog of the integral equation of Kirkwood

$$-kT \ln[g(r_{12})] = u(r_{12}) + \Gamma \int_{(A)} u(r_{13})g(r_{13})[g(r_{13}) - 1] \, dA_3 \quad (59)$$

accounts through the correlation function g for the fluid structure, multiple collisions and interaction energy and can be used to derive the EOS. As it is usual when solving such problems we used several approximations, the most important ones being the use of the sticky potential and expansion of the correlation function in series up to linear terms in β (in ref. [25] the same approximation was used):

$$g(r) = g_{hc}(r) + \frac{w}{kT} g_1(r) + \cdots \quad (60)$$

We succeeded to obtain an EOS which confirmed the coefficients 4β and $32\beta^2$ in Eq. (55) for small and moderate θ's.

5. Data processing

The experimental data for $\sigma = \sigma(C_s)$ were processed by numerical simultaneous solution of the equations of the adsorption isotherm and the equation of state. They are obtained experimentally as a set of values $\sigma^{\exp}(c_k)$ for $k = 1, 2, \ldots, N$, where N is the number of experimental points. The value of the interfacial tension of pure solvent, σ_p, is known and therefore, the input data for the numerical procedure are the values of the surface pressure $\Delta\sigma^{\exp}(c_k)$ for $k = 1, 2, \ldots, N$. If we choose some trial values for the model parameters (α, β and K_s), then for each concentration, c_k, we can calculate the adsorption, $\Gamma^{th}(c_k)$, predicted from the adsorption isotherm. The adsorption isotherms are represented by monotonic functions (except for the cases of phase transition). For that reason we use the simplest bisection method for numerical solution of the transcendental equations describing the adsorption isotherms. Substituting the calculated value of $\Gamma^{th}(c_k)$ into the equation of state we calculate the prediction for the surface pressure $\Delta\sigma^{th}(c_k)$. Such procedures has a useful "bi-product"—it gives as intermediate result the dependence $\Gamma(C_s)$, which can be used for calculation of the EOS $\Delta\sigma$ vs Γ and the Gibbs elasticity.

The adjustable parameters (α, β and K_s) are determined by means of the least-squares method, that is, by numerical minimization of the merit function

$$\chi^2(\alpha, \beta, K_s) = \frac{1}{N} \sum_{k=1}^{N} [\Delta\sigma^{\exp}(c_k) - \Delta\sigma^{th}(c_k; \alpha, \beta, K_s)]^2 \quad (61)$$

assuming that all experimental points have equal errors. The minimization algorithm is simple. We define relative steps (s_α, s_β, s_K) of model parameters. Starting from a given point (α, β, K_s) we define all points in the $3 \times 3 \times 3$ local grid around (α, β, K_s) with absolute steps ($s_\alpha\alpha, s_\beta\beta, s_KK_s$) and calculate the values of the merit function. We compare all 27 values in order to find the position of the local minimum, change the initial guess with the obtained position, and repeat the procedure again. The algorithm stops when the initial guess and the obtained position of the local minimum coincide. This simple procedure gives possibility to calculate the position of the global minimum χ_{min} of the merit function.

One problem we encountered with the generalized HFL isotherm, Eq. (56), was that it contains a power $(1 + 8\beta)/(4\beta)$, which diverges for $\beta = 0$ and makes the fit uncertain for small β. To avoid or at least to decrease this problem we transformed the logarithm

of the singularity term as follows:

$$\frac{1}{4\beta} \ln\left(\frac{2}{1 + R_\beta}\right) = -\frac{1}{4\beta} \ln\left(1 + \frac{R_\beta - 1}{2}\right) = -\frac{1}{4\beta} \ln(1 + \xi)$$

$$\text{with } \xi \equiv \frac{8\beta}{1 + R_\beta} \frac{\theta}{1 - \theta} \quad (62)$$

leading to

$$\frac{1}{4\beta} \ln\left(\frac{2}{1 + R_\beta}\right) = -\frac{2}{1 + R_\beta} \frac{\theta}{1 - \theta} \left(1 - \frac{\xi}{2} + \frac{\xi^2}{3} - \frac{\xi^3}{4} + \cdots\right) \quad (63)$$

In the new expression β appears in the nominators and there is no divergence.

6. Numerical results and discussion

We decided to check and compare all adsorption equations discussed above with two types of surfactant: (i) several homologues of the dimethyl alkyl phosphine oxide DMPO: C8, C10, C12 and C14 from ref. [26] and C8, C9, C10, C11, C12 and C13 from ref. [27]; and (ii) aliphatic acids: C7, C8 and C9 from ref. [28] and C10 from ref. [29]. The reason for this choice was our desire to investigate the role of different factors. The DMPO's are typical surfactants with large hydrophilic groups, which are supposed to interact between themselves only by steric repulsion, whereas the acids are known to form strong hydrogen bonds and to remain dimerized even in gas phase. For the sake of brevity we will use the following abbreviations for the names of the models: the first capital letter indicates the model equations are based upon (H for HFL, V for Volmer and L for Langmuir). If it is followed by G, it means that we are using the generalized isotherm or EOS for the respective model. When it is followed by a number, it indicates the number of free parameters involved (2 or 3), e.g. H–G means generalized HFL, Eq. (56), and V–3 means Volmer model with 3 parameters, Eq. (8). We must point out that all fits were practically perfect—most had regression coefficients $R^2 = 0.999$ or 0.9999 and only a few were with 0.997 or alike. In spite of the good fits couple of substances gave somewhat strange results and we discarded them from the numerical calculations, although we kept them in the table—this refers to the C8 and C10 DMPO from both series. The reason for this could be purely mathematical (see Appendix A), although we suspect also some physical reasons, but could not prove them beyond doubt.

Because of the numerous data, we did not present all results graphically, especially when they were similar. Although all groups of data lead to similar or even identical results, in most numerical calculations with DMPO we used the data of ref. [27] simply because they were more numerous. Typical fits of the adsorption isotherms $\sigma = \sigma(C_s)$ and the equations of state $\Delta\sigma = \Delta\sigma(\Gamma)$ are presented in Figs. 8 and 9 (for clarity the fitting curves in Fig. 9 are not shown). The numerical results obtained from the fits of the adsorption isotherms for all considered above six models are presented in Table 2 (for DMPO) and 3 (for acids). We processed also all EOS, which gave practically identical data with the adsorption isotherms for the parameters α and β. Only for illustration of this statement in Table 2 we presented the results obtained with the EOS from the model H–G with DMPO, which can be compared with the results in the adjacent column H–G, obtained by the adsorption isotherm.

Even superficial inspection of the data in Tables 2 and 3 allows some interesting conclusions.

(i) Practically all 6 models lead to identical (although slightly scattered) values of the adsorption constant K_s. This should not be surprising since K_s is present only in the left hand side of the adsorption isotherms. Indeed, if in all adsorption isotherms

Table 2
Parameters from the fit with seven equations of the data for adsorption of alkyl di-methyl phosphine oxides (DMPO) at Air/Water interface (K_s: adsorption constant; α: minimum area per molecule; β: interaction constant); H–G: EOS Eq. (54); H–G Eq. (56); V–G Eq. (48); H–3 Eq. (16); V–3 Eq. (8); L–3 Eq. (13).

Surfactant	Parameters	EOS–G	H–G	V–G	L–G	H–3	V–3	L–3
C8–DMPO [26]	$K_s \times 10^4$, (cm)	–	8.30	8.56	7.85	9.23	8.58	7.84
	α (Å^2)	24.0	26.70	36.17	47.92	18.61	31.20	47.92
	β	0.14	0.28	0.18	0.01	0.14	0.09	0.01
C8–DMPO [27]	$K_s \times 10^4$, (cm)	–	11.41	10.71	9.33	11.86	10.77	9.32
	α (Å^2)	24.5	23.91	35.09	48.80	19.84	32.55	48.80
	β	0.13	0.12	0.08	0.00	0.03	0.00	0.01
C9–DMPO [27]	$K_s \times 10^4$, (cm)	–	20.46	23.78	23.94	20.56	23.12	23.92
	α (Å^2)	31.0	31.33	41.91	45.95	24.40	34.21	45.95
	β	0.52	0.61	0.55	0.08	4.16	1.25	0.08
C10–DMPO [26]	$K_s \times 10^4$, (cm)	–	83.50	88.44	73.93	91.32	83.65	74.46
	α (Å^2)	18.9	25.80	31.50	43.17	19.56	30.78	43.23
	β	0.01	0.29	0.06	0.01	1.03	0.42	0.01
C10–DMPO [27]	$K_s \times 10^4$, (cm)	–	81.90	81.30	71.77	79.37	85.03	71.83
	α (Å^2)	24.49	25.04	35.29	42.71	20.44	29.39	42.71
	β	0.20	0.27	0.25	0.01	2.05	0.06	0.01
C11–DMPO [27]	$K_s \times 10^4$, (cm)	–	116.4	165.7	172.0	133.0	144.0	171.7
	α (Å^2)	30.02	30.04	38.65	40.59	22.62	31.96	40.69
	β	1.15	1.25	1.05	0.78	6.13	2.81	0.74
C12–DMPO [26]	$K_s \times 10^4$, (cm)	–	429.0	583.0	634.5	500.9	548.1	639.5
	α (Å^2)	29.8	30.30	39.66	41.01	22.61	31.89	40.96
	β	1.02	1.23	1.14	0.73	5.92	2.61	0.67
C12–DMPO [27]	$K_s \times 10^4$, (cm)	–	300.0	475.0	508.4	402.0	440.3	524.4
	α (Å^2)	33.34	33.45	42.77	44.15	24.52	34.55	44.06
	β	1.76	1.97	1.74	1.59	7.24	3.55	1.34
C13–DMPO [27]	$K_s \times 10^4$, (cm)	–	612.2	982.0	1066	842.1	927.4	1061
	α (Å^2)	27.90	27.90	35.68	36.73	20.38	28.69	36.98
	β	1.93	2.07	1.82	1.63	7.33	3.59	1.48
C14–DMPO [26]	$K_s \times 10^4$, (cm)	–	3740	5972	6273	4629	5142	6048
	α (Å^2)	30.7	31.00	38.64	40.38	23.02	32.15	40.81
	β	1.31	1.51	1.10	0.80	6.52	2.95	0.88

we set $\alpha = \beta = 0$, they will all give the same result-Henry's law $K_S C_S = \Gamma$, which is of course model independent.

(ii) The two models, based on Langmuir isotherm L–G and L–3, lead for DMPO practically to the same values of the adsorption parameters. This confirms our theoretical considerations in Section 4.1 that for small values of β the Frumkin equation becomes exact for localized adsorption. The situation is however somewhat different with the acids in Table 3, where β can be as large as 6.

(iii) The area per molecule, α, determined by the generalized equations H–G, V–G and L–G increases in this order, as anticipated in Section 3.2. However, their ratio is not 1/2/4 as it must be for $\theta \to 0$ according to the theory, because the fit gives some averaged value for all concentrations—for the lower homologues the ratio is approximately 1/1.3/2, but for the higher homologues it becomes 1/1.3/1.3, which is in agreement with the behavior of the curves at $\theta \to 1$ in Fig. 3.

(iv) The simplified equations, Eqs. (8), (13) and (16), lead to smaller values of α and larger values of β (in a correlated manner) with respect to the values from the generalized equations. For example, the values of α, obtained by the approximate van der Waals equation V–3 are lower than the values obtained with the respective exact equation V–G, which in turn are much larger than the values, obtained with the 2D equation H–G. As a result the values of α obtained by V–3 become closer (but still remain larger by 10–25%) to the presumably true values,

Table 3
Parameters from the fit with seven equations of the data for adsorption of aliphatic acids at Air/Water interface (K_s: adsorption constant, α: minimum area per molecule, β: interaction constant); H–G EOS Eq. (54); H–G Eq. (56); V–G Eq. (48); H–3 Eq. (16); V–3 Eq. (8); L–3 Eq. (13).

| Surfactant, [ref.]	Parameters	EOS–G	H–G	V–G	L–G	H–3	V–3	L–3
C7–acid [28]	$K_s \times 10^4$, (cm)	–	0.906	1.46	1.68	1.53	1.58	1.82
	α (Å^2)	22.9	23.1	30.0	30.5	16.5	23.6	30.5
	β	2.97	3.38	3.55	3.44	8.54	4.67	2.51
C8–acid [28]	$K_s \times 10^4$, (cm)	–	1.76	2.20	3.16	3.63	3.73	3.90
	α (Å^2)	15.1	18.1	27.9	29.3	14.5	21.5	29.8
	β	3.26	6.26	10.3	6.91	10.4	6.02	3.58
C9–acid [28]	$K_s \times 10^4$, (cm)	–	9.52	15.5	18.4	16.9	18.4	20.7
	α (Å^2)	20.9	21.8	28.6	29.1	15.7	22.3	29.1
	β	3.04	4.18	4.65	4.27	9.31	5.03	2.66
C10–acid [29]	$K_s \times 10^4$, (cm)	–	16.8	30.0	42.3	41.8	45.7	51.2
	α (Å^2)	20.2	21.9	28.5	28.8	15.6	22.1	28.8
	β	4.28	7.55	8.58	6.07	10.5	5.86	3.30
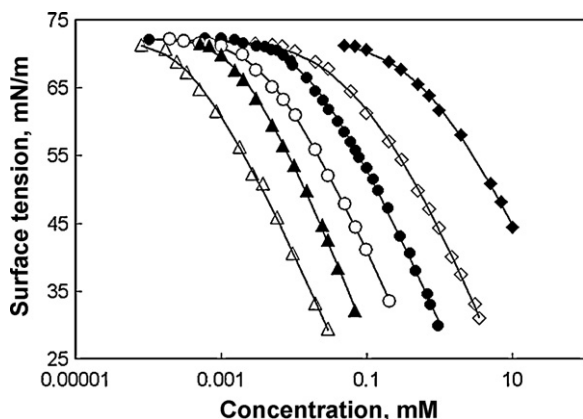
Fig. 8. Fit by model H–G of the curves surface tension vs. surfactant concentration for the DMPO surfactants—◆: C8; ◇: C10; ●: C11; ○: C12; ▲: C13; △: C14.
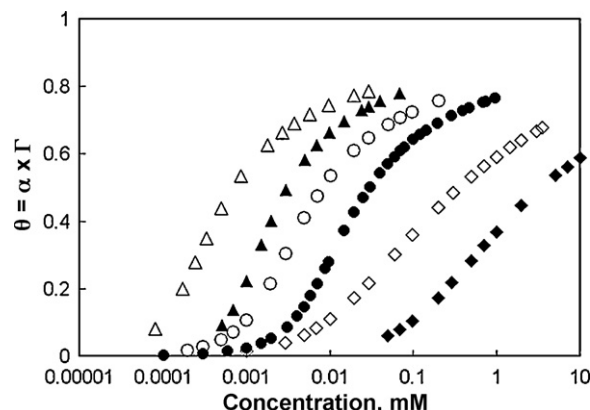

Fig. 10. Degree of coverage θ vs. DMPO concentration from model H–G (same symbols as in Fig. 8).

obtained from H–G (see Tables 2 and 3) thus creating the wrong impression that V–3 might be a correct equation. However, this decrease is not uniform for all DMPO's and it is not clear how large the error is. The reason for this behavior can be understood by comparing curves E2 (for the exact equation V–G) and A2 (for the approximate V–3). For example, value of the abscissa $\alpha\Gamma \approx 0.5$ corresponds to ordinate 0.5 for E2, but to 0.75 for A2. In order to obtain the correct value of the ordinate 0.5 from A2 one must choose $\alpha\Gamma \approx 0.4$, which can be achieved only by decreasing α by 25%. The coordination between α and β is analyzed in Appendix A. The same effects are observed with all approximate models. For instance, α drops for the approximate model H–3 even below 20 Å^2, while β reaches the incredible values of 6–7.

Truthful to our philosophy, presented in Introduction, we did everything possible to check at least some results of the fits by independent methods or data. We are not aware of a method allowing direct determination of the most important parameter α. However, this information can be extracted from the EOS of C18–DMPO measured by Noskov et al. [30]. From their curves one can deduce that the collapse point of the monolayer corresponds to area 34 Å^2. Assuming that at this area the packing was closed hexagonal and knowing that the area of the inscribed circle is 0.906 of that of the hexagon, one finds $\alpha = 30.8$ Å^2, which is practically equal to the values obtained by us by the method H–G for the DMPO's above C10. It is very probable that the other few DMPO have the same area. As for the acids, the values obtained (except for C8) between 20 Å^2 and 20.9 Å^2 hardly need verification, since this is the cross-sectional area of the paraffinic chain.
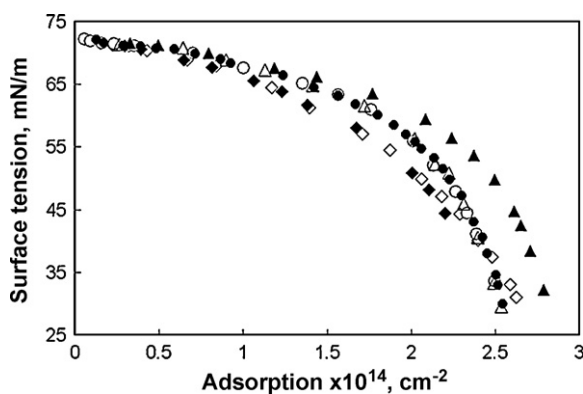
We used the H–G data for α to calculate the degree of coverage of the surface. The data are shown in Figs. 10 and 11. As one sees, the degree of coverage $\theta = \alpha\Gamma$ is significantly lower than unity even at the highest concentrations. This result cast doubt on the common belief that before and close to the critical micelle concentration CMC the degree of coverage is complete. We believe that this finding may have some technological significance.

The values of the adsorption constants K_s can be checked from the slope of the initial portions of the plots of σ vs. C_s. This procedure is extremely difficult since the concentrations are very small and the data for σ are not very reliable (the authors of [27] also mentioned this problem). To decrease the possible errors we were drawing a line though the point ($C_s = 0, \sigma_p$), where σ_p is the surface tension of the pure solvent and were trying to find several data points lying on this or close to this line. Examples of this procedure are given in Figs. 12 and 13. The adsorption constant is calculated by combining Gibbs' equation and Henry's law $\Gamma = K_{s,c}C_s$, where the subscript c indicates that the constant is calculated in this way The result is

$$K_{s,c} = -\frac{kT}{(\partial\sigma/\partial C_s)_{in}} \tag{64}$$

where "in" stands for "initial". In Figs. 14 and 15 the respective results for K_s of DMPO's and acids are plotted vs. the number of carbon atom in the chain n_c along with the results in columns H–G, V–3 and L–3 of Table 2 obtained by fits with the respective equations. As already mentioned, although not coinciding, the results are reasonably close and follow rather well straight lines, see Eq.

Fig. 9. Equation of state of DMPO surfactants from model H–G (same symbols as in Fig. 8).
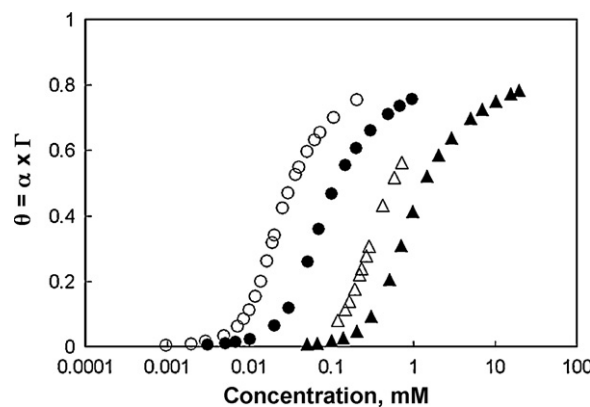

Fig. 11. Degree of coverage θ vs. acid concentration from model H–G—▲: C7; △: C8; ●: C9; ○: C10.
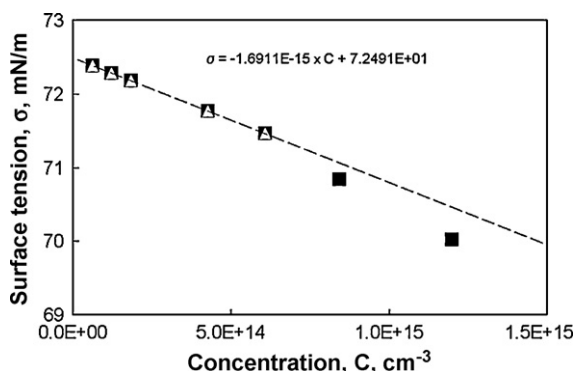
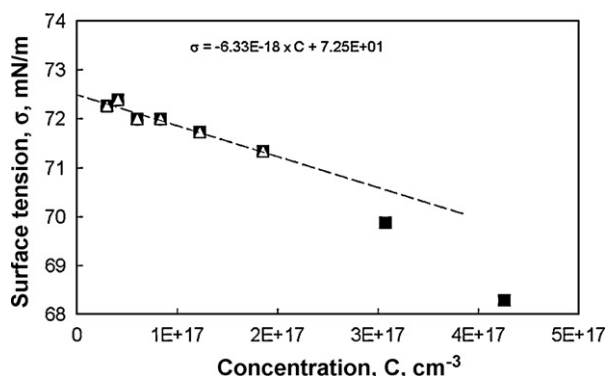**Fig. 12.** Initial portion of the curve surface tension vs. C12 DMPO concentration. The equation is shown in the figure.

Fig. 13. Initial portion of the curve surface tension, σ, vs. heptanoic acid concentration, C_s. The equation is shown in the figure.

(9):

$$\ln K_s = \frac{w_c}{kT} n_c + Q \qquad (65)$$

The points are so close, that it was impossible to draw separate lines. Hence, we summarized the values of the slopes $w_c/(kT)$, the intercepts Q and the regression coefficients r^2 of the lines in Table 4. We assumed that the most probable slope is 0.96 although the average value is 0.951. The slope of this dependence was determined also by Davies and Rideal [19], who found slightly larger value: $w_c/(kT) = 1.02$.
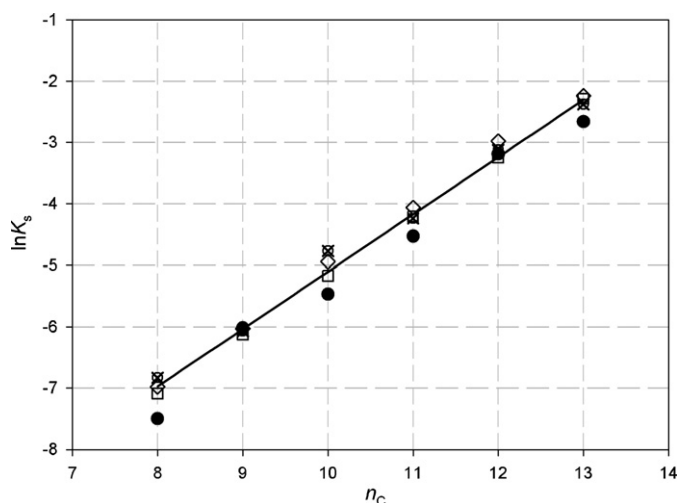

Fig. 14. $\ln K_s$ (adsorption constant) vs. number of carbon atoms n_c for DMPO surfactants. The average line has the following parameters: slope 0.933, intercept −14.43 and $r^2 = 0.9862$. The numerical data and the symbols are given in Table 4.
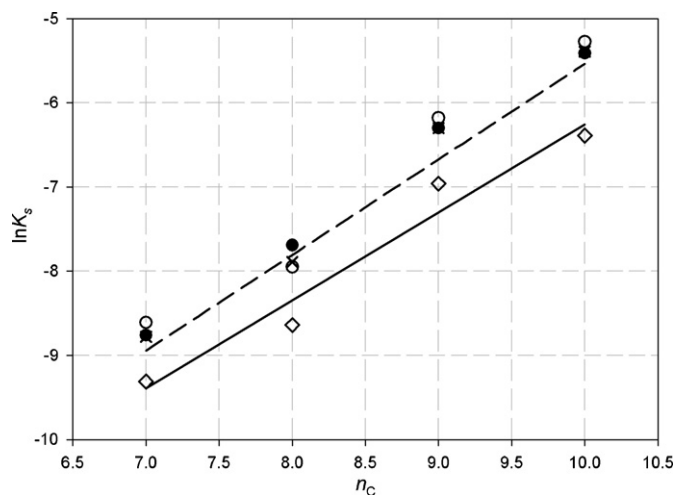

Fig. 15. Plot of $\ln K_s$ for aliphatic acids vs. the number of carbon atoms n_c. The symbols are the same as in Table 4. For the parameters of the linear fits see the text.

The data for acids are slightly worse and more scattered than those for DMPO. The average slope of all data in Fig. 15 (the dashed line) is $w_c/(kT) = 1.135$ (slightly larger than that for DMPO) and the intercept is −16.89. There is no reason however that the adsorption energy of the methyl groups in both types of compounds be different. We attribute this difference to the lower precision of the data, the more so that the data obtained with the model H–G (the solid line) gives a lower slope, 1.044 with intercept −16.70.

We decided to use these data to check the correctness of our theoretical Eq. (9) for K_s. Besides the slope $w_c/(kT) = 0.96$ we used the following data: $\sigma_p = 72.2$ mN/m, $\alpha_c = 20$ Å^2 and $\delta_s = 1.16 \times 10^{-8}$ cm [9]. In fact, the theoretical results were already plotted in Fig. 14 as $\ln K_s$ vs. n_c (see also Table 4). The agreement with the other data in Fig. 14 is very good. Another way to check Eq. (9) is to calculate theoretically the intercept $Q = \ln \delta_s + \sigma_p \alpha_c/(kT)$. The result is −14.76, which is almost equal to the value −14.66 obtained from the fit by the H–G method. The final check of the reliability of our Eq. (9) was the direct comparison of the results it leads to with the data, obtained by fitting the experimental isotherms by the method H–G. Fig. 16 demonstrates almost perfect agreement between the theoretically calculated values K_s^{th} and the ones obtained from the experimental data, $K_s^{H–G}$.

The last constant to be checked is β. We have assumed during the derivation of Eq. (33) that the chains are perpendicular to the interface, but at the same time showed in Eq. (19) that the first methyl group is immersed in the solution. Therefore, these groups can interact only though the water, which significantly weakens the interaction [11] and we will neglect them as we did when deriving Eq. (20). However, in the present case the top cover on the molecule does not take part in the interaction, so that the number of interacting methyl groups will be $n_c - 1$. The situation with the acids is even more complicated. The first carbon atom is in fact that of the carboxyl group and it is certainly immersed. The second one should

Table 4
Parameters of the linear fits of the data for the dependence of the adsorption constants K_s of DMPO compounds on the number of carbon atoms n_c, obtained by five methods (see table).

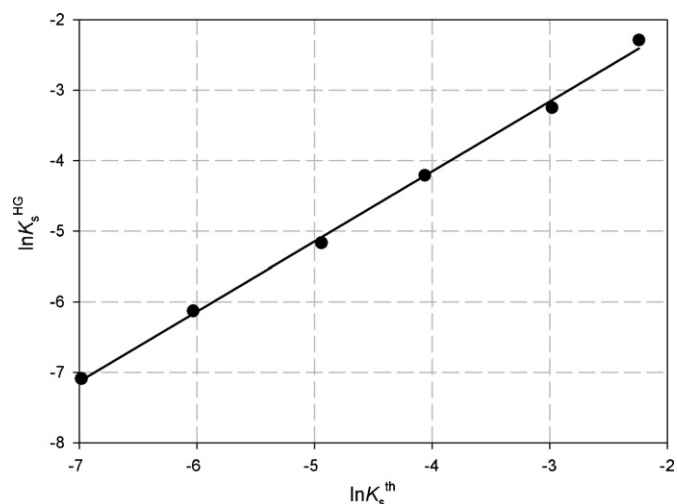| Symbol	Model/(Eq.)	$w_c/(kT)$	Intercept Q	r^2
●	$\sigma(C_s)$ (64)	0.961	−14.98	0.9841
■	Theory (9) and (20)	0.960	−14.77	1.0000
◇	Fit H–G (56)	0.964	−14.66	0.9979
×	Fit V–3 (8)	0.904	−14.06	0.9922
○	Fit L–3 (13)	0.967	−14.69	0.9974

Fig. 16. Linear dependence between the logarithms of the theoretical K_s^{th} and the experimentally obtained by the model H–G value K_s^{H-G} of the adsorption constants or DPMO surfactants. The parameters of the fits are: slope 1.004 and intercept −0.170.

Fig. 17. Values of the interaction constant, β, vs. the number of carbon atoms n_c. for DMPO surfactants. The dashed line is only for guiding the eye. The theoretical values, calculated from Eq. (67) are with solid line. The experimental values (with dashed lines and empty symbols) are calculated from the fit of the experimental data by the model H–G.

be also immersed (as the first one of the DMPO) not only because of Eq. (20), but because of the mere fact that the acetic acid is infinitely soluble in water. Therefore, for acids the interacting methyl groups must be $n_c - 2$. We will denote the number of interacting groups by n_{int}.

Since some of the molecules have short chains and large area α of the polar head, it is possible that the length l and the diameter d have close values. That is why we will not use the simple Eq. (35), but the exact one, Eq. (33), which we will rewrite in slightly different form:

$$\beta = \frac{0.75\pi\rho_t^2\alpha_p I}{4d^2\alpha kT}\frac{l}{d}\arctan\left(\frac{l}{d}\right) \tag{66}$$

We determined the values of the parameters of a methyl group from the properties of the paraffinic compounds [18,32]: $l = l_1 n_{int}$; $l_1 = 1.27\,\text{Å}$; $\rho_t = 1/l_1$; $\alpha_p = 2\,\text{Å}^3$; $I = 10.5\,\text{eV}$. After some calculations we thus found:

$$\beta = 510\frac{n_{int}}{\alpha^{5/2}}\arctan\left(\frac{1.12n_{int}}{\alpha^{1/2}}\right) \tag{67}$$

where $n_{int} = n_c - 1$ for DMPO and $n_c - 2$ for acids.

As we already mentioned, with the exception of $\ln K_s$, the data for the DMPO compounds C8, C10 (and to some extent C13) exhibit some deviations from the trend followed by the other data (for additional discussion see Appendix A)—the values of α are with 10–15% lower than for the other compounds and the values of β also deviate considerably from the general trend (see Table 2). That is why we performed calculations of β only for the other compounds. In Fig. 17 the results for β obtained from the fit of the experimental data by the method H–G (we call them "experimental") are compared with the respective theoretical calculations of β by Eq. (67). The scattering of the data points for the H–G isotherm with respect to the theoretical curve β vs. n_c, calculated from Eq. (67) do not exceed 15–25%, which is very close to the usual error of determination of β. Note that again this is result of direct calculation without using any adjustable parameter. The (moderate) success of this procedure is rather surprising, in view of the crudeness of the theoretical model and the lack of relevant data.

Parallel comparison of results between several models is performed in Fig. 18, where the "experimental" and the theoretical values of β vs n_c are plotted together for the three models: H–G, V–3 and L–3. The coincidence between theory and experiment for the model L–3 in Fig. 18 is pretty good, but this result might be
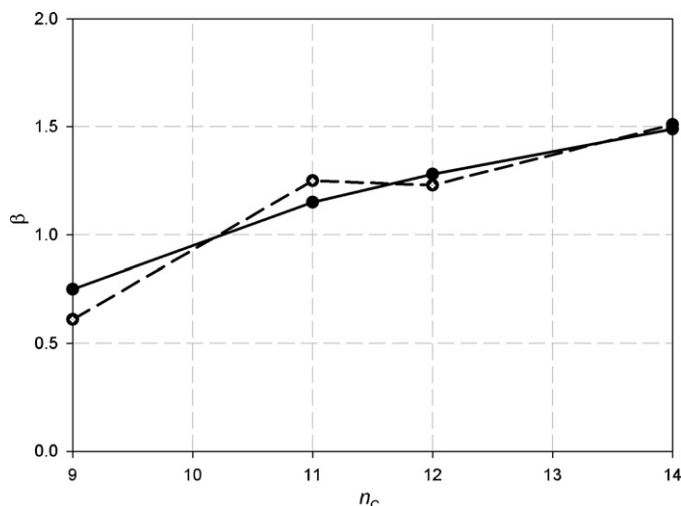
misleading. The values of β for this model are very small (<0.5) and the values of α (which in Eq. (67) is in the denominator as $\alpha^{5/2}$) are very large (see Table 2), which might be the reason for this coincidence. If one calculates the theoretical values for L–3 of β by using the presumed true values of $\alpha \approx 30\,\text{Å}^2$, they will become larger than 1 and the coincidence between theory and experiment for L–3 will vanish. As for the model of Volmer V–3, the difference between experimental and theoretical values is enormous-up to 5–6 times, which confirms the data from Table 2, showing that this model exaggerates the values of β.

Although the results for β are not excellent, we will dare some speculations. The fact that Eq. (67), which works rather well, was derived from the second virial coefficient, accounting only for binary interactions between molecules, perpendicular to the interface, seems to suggest that this is the dominant orientation of interacting molecules even at low surface
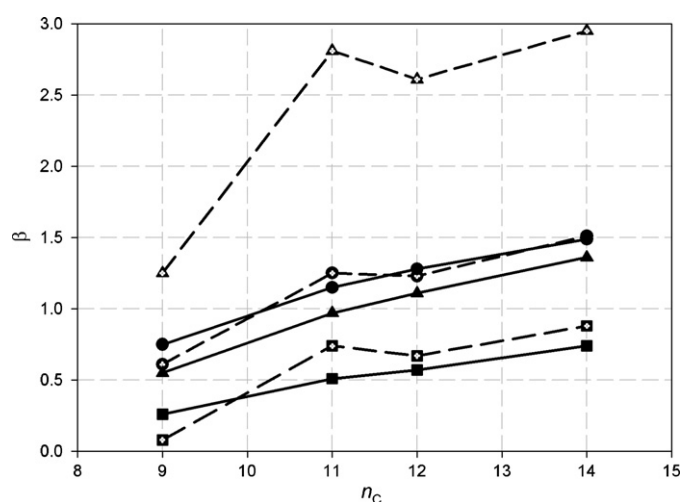

Fig. 18. Values of the interaction constant, β, vs. the number of carbon atoms n_c. for 4 DMPO surfactants (see the text). The dashed lines are only for guiding the eye. The theoretical values, calculated from Eq. (67) are with solid lines with values of α, corresponding to do respective model, indicated on the right. The experimental values (with dashed lines and empty symbols) are calculated from the fit of the experimental data by the models H–G [circles; Eq. (16)], L–3 [squares, Eq. (13)] and V–3 [triangles, Eq. (6)].
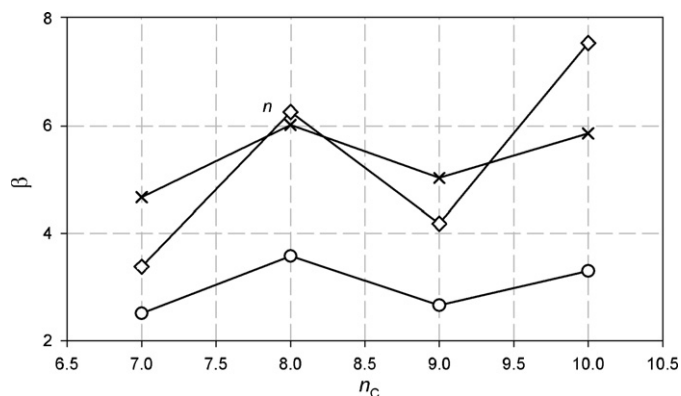
Fig. 19. Experimental results for the parameter, β, vs. number of carbon atoms n_c for aliphatic acids, obtained by fitting the data with three models; H–G, V–3 and L–3 (see symbols in Table 4). The dashed lines are only for guiding eye. See text for discussion.

concentrations—probably the attraction between the hydrocarbon tails is the dominant effect trying to decrease the free energy of the surfactant molecules by forcing them to stay as close as possible to each other. This is also in agreement with the fact that the area per molecule α, determined by the fit of the model H–G leads to values of α very close to those determined from the collapse pressure of DMPO (see above). Such effect is possible however only if the molecular length l exceeds considerably the distance of closest approach d. For example for C12 the ratio is $l/d \approx 2.5$. On the contrary, for short molecules like C8 this ratio is close to 1 and since l is small the attraction is too weak to orient the molecules vertically. This might be one of the reasons for the small values of β for short molecules.

The experimental results for β vs. n_c in Fig. 19 for acids look very differently from those for DMPO. First, the values of β are much larger, which is probably due to the strong hydrogen bonding. More important is the observed saw-shape of the curves. It looks a little bit as the well known dependence of the melting point of alkanes and the reason might be the same. With alkanes the substances with even number of carbon atoms are supposed to be more able to acquire in the solid phase conformations with higher attractive energy, which leads to higher melting point. Some similar, but probably more complicated effect is possible in the adsorbed layer. Indeed, the very small values of $\alpha \approx 21$ Å^2, which is very close to the cross-sectional area of the paraffinic chain, may lead to interpenetration of the chains, making their structure similar to that in solid phase with alkanes more strongly attracting for even number carbon atoms which manifests itself here by larger values of β. Another possible effect is the change of acidity of the carboxylic groups with the chain length, which may lead to vertical displacement and change of density of the adsorbed layer—similar effect of ions on alkanes was investigated in [31]. This is of course a speculation, which can hardly be proven.

Unfortunately, no comparison between the models by direct fit of the experimental data for σ vs C_s is possible, because as already mentioned, all models fit perfectly the experimental data but lead to different system parameters. The different behavior of the models can be however demonstrated by plotting the Gibbs elasticity E_G and the degree of surface coverage $\theta = \alpha \Gamma$ vs. the surfactant concentration C_s. This is done in Figs. 20 and 21 for the generalized versions of the three models. As one might expect, the fact that the model H–G corresponds to the smallest values of α leads to considerably smaller values of E_G and θ.

We consider the results, presented in this section, especially those with DMPO (which are also due to the excellent experimental data from refs. [26,27]), as confirmation not only of our new
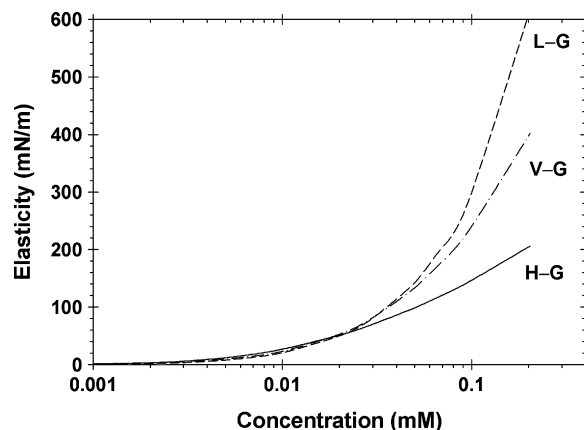

Fig. 20. Gibbs elasticity as a function of surfactant concentration for DMPO–C12 calculated from models L–G, V–G, and H–G.
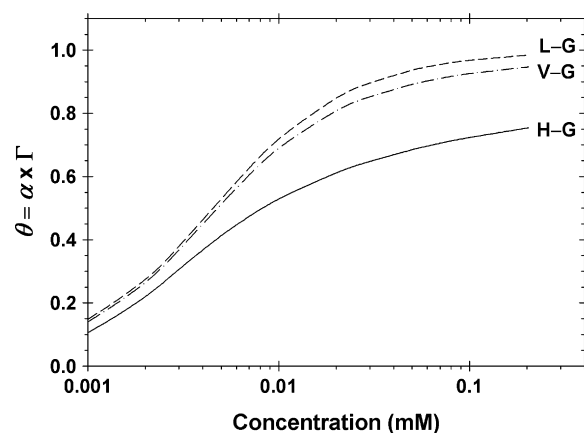

Fig. 21. Degree of surface coverage, θ, as a function of surfactant concentration for DMPO–C12 calculated from models L–G, V–G, and H–G.

adsorption isotherm, Eq. (56) and the EOS Eq. (54), whose fit gave the above values, but also as confirmation of our equations for the adsorption energy E_A, Eq. (20), thickness of the adsorbed layer δ_s, Eq. (21), and the adsorption constant K_s, Eq. (9). It is noteworthy that we obtained these results without using during the calculation any adjustable parameters.

7. Conclusion

We carried out analysis, based on the three most popular simple equations with three free parameters (adsorption constant K_s, minimum area per molecule α and interaction constant β) of surface tension isotherms of DMPO and aliphatic acids. It revealed more or less the same problems which we met in [9] with ionic surfactants. This stimulated us to look again on the expressions and the values of α, K_s and β. In [9] we have shown that correct results can be obtained only if the hard core part of the EOS is based on the model of HFL (see Section 3.b). We had also significantly modified the expression for K_s by introducing new terms in the expression for the adsorption energy E_A, Eq. (20), and derived a new expression for the thickness of the adsorbed layer, δ_s. The new modification we introduced now are the calculations of the average immersion depth z_{imm} of the paraffinic chain due to thermal fluctuations, Eq. (19), which affects E_A and β, and of the parameter β by integrating the interaction energy between two paraffinic chains, Eqs. (33) and (66). In this way we prepared the ground for independent verification of the parameters determined by the fit of the experimental data surface tension σ vs. surfactant concentrations C_s. However,

our results from such fits, (see Tables 2 and 3), showed that again the values of the parameters determined were not only strongly dependent on the model used, but were in most cases different from the independent theoretical estimates.

The conclusion we reached was that the poor results are due to the models used (the EOS and the adsorption isotherm). That is why we tried to use also or to derive equations as precise as possible. An almost exact generalization of the Langmuir–Frumkin equation was available, see Eqs. (36) and (37) and [13]. However, nothing was available for fluid monolayers. We succeeded to derive an exact EOS, Eq. (48), for 1D adsorption of sticks on a thread by using the so-called "sticky approximation" of Baxter [21] assuming that attraction between the molecules appears only when they touch each other. Our result turned out to be a generalization of Volmer equation, since its hard core part exactly coincides with that of Eq. (6). Since we have proven that the Volmer equation leads to values of α larger than the true ones (see Fig. 3), the new equation must have the same defect. On the other hand, it has been rigorously proven [21] that it is impossible to derive a 2D EOS even for hard discs, let alone for attracting each other disks. Hence, we used a heuristic approach: we derived rigorously a 2D generalization of the HFL equation with correction up to linear in β terms, see Eq. (53), and changed suitably the hard core part and the numerical coefficients in the 1D equation to make it compatible with the new 2D result. The numerical checks of the new equation, Eq. (54), and the respective adsorption isotherm, Eq. (56), were performed by calculating the third virial coefficient and by deriving an analogous equation by expansion of the correlation function in series of β and solving Kirkwood's integral equation. Both checks gave satisfactory results.

We subject the three simple equations (more precisely the respective adsorption isotherms) from Section 2, Eqs. (8), (13) and (16), and their respective generalized analogs Eqs. (37), (50) and (56) to experimental checks by fitting the data of Makievski and Grigoriev [26] and Warszynski and Lunkenheimer [27] for DMPO and of Malysa et al. [28] and Lunkenheimer and Hirte [29] for acids. The results are summarized in Tables 2 and 3. They show that practically all 6 models lead to close (although slightly scattered) values of the adsorption constant K_s. This should not be surprising since K_s is present only in the left hand (model independent) side of the adsorption isotherm. The two models, based on Langmuir isotherm, lead for DMPO practically to the same values of the adsorption parameters. This is so because only the second virial coefficient contains a term linear in β and in all other terms β is at higher power. For small β (which is the case with DMPO) these terms can be neglected and Frumkin equation becomes *from this view point* exact (see Section 5a)—however, the problems with the exaggerated values of α remain. The situation is however different with the acids, where β can be as large as 4 and the two equations lead to different results.

The area per molecule α, determined by the generalized equations increases from HFL to Volmer to Langmuir, as anticipated in Fig. 3. The simple equations leads to smaller α and larger β (in a correlated manner) with respect to the values from the generalized equations. We showed, by using the data of Noskov et al. [30] that the values of $\alpha \approx 30\,\text{Å}^2$ given in Table 1 by the generalized HFL model are very close to the geometrical area of the DMPO heads.

We performed several independent calculations of the three adsorption parameters in order to compare the results with those obtained by the fits and to check in this way our theoretical developments and the reliability of our fitting procedures. The first one was to calculate K_s directly from the initial slope of the experimental curves $\sigma(C_s)$ (see Figs. 12 and 13). The data were rather scattered but the result, shown in Table 4 was in agreement with the other data. The other test was direct calculation by the method H–G of the adsorption constant K_s from Eq. (9) without use of any adjustable

parameter. Finally, we calculated the constant β from Eq. (67) again without using adjustable parameters. The best results were again obtained by the method H–G (see Figs. 16 and 17). The experimental results with acids for β vs. n_c in Fig. 19 look very differently from those for DMPO. First, the values of β are much larger, which is probably due to the strong hydrogen bonding. More important is the observed saw-shape of the curves. We have no explanation for this, but we suspect that similarly to the dependence of the melting point of paraffins on n_c, it is due to the better capability of the substances with even number of carbon atoms to acquire conformations with higher attractive energy.

In conclusion, we believe to have shown that the new EOS, Eq. (54), and adsorption isotherm, Eq. (56), derived by us have given very reliable results. However, we are aware that no definite conclusion is yet possible without check with other suitable systems and without more rigorous derivation and possibly improvement of our equations. At the same time our analysis has demonstrated that the other equation tested, those of Frumkin and van der Waals qualitatively correctly describe the adsorption phenomena. Moreover, they are simpler and more easy for applications, so that if one is interested mainly in qualitative comparison of surfactants or in the general features of the phenomena observed, they might be preferable. If however one wants to obtain more information for the value of some parameter, one must be cautious in the selection of the method to be used.
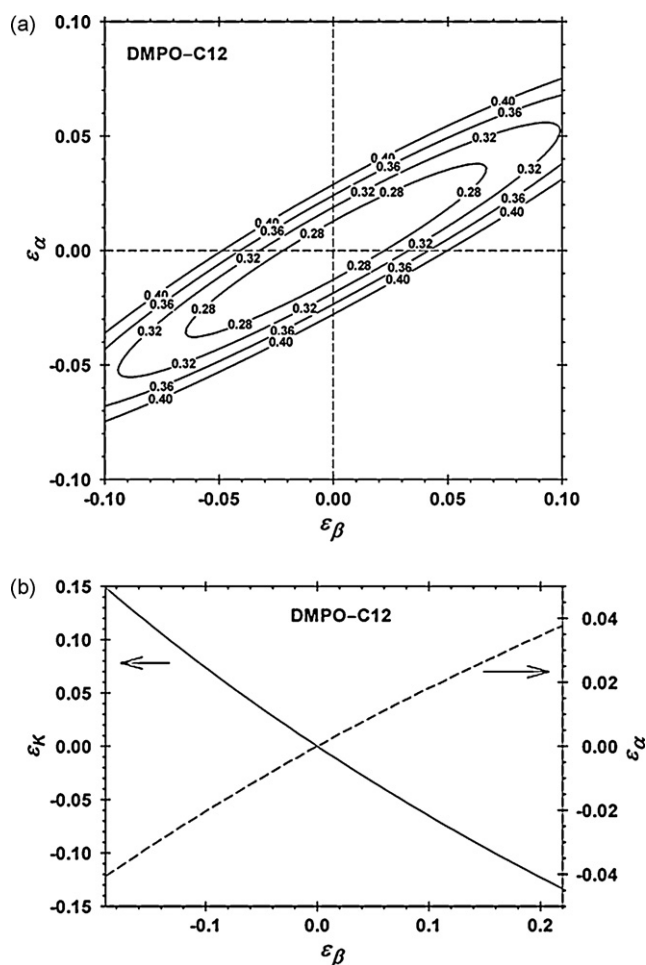

Fig. A.1. Results from processing of experimental data for DMPO–C12 using H–G model. (a) Contour plot of the merit function for fixed $K_{s,\text{min}}$; (b) change of ε_K and ε_α as a function of ε_β.
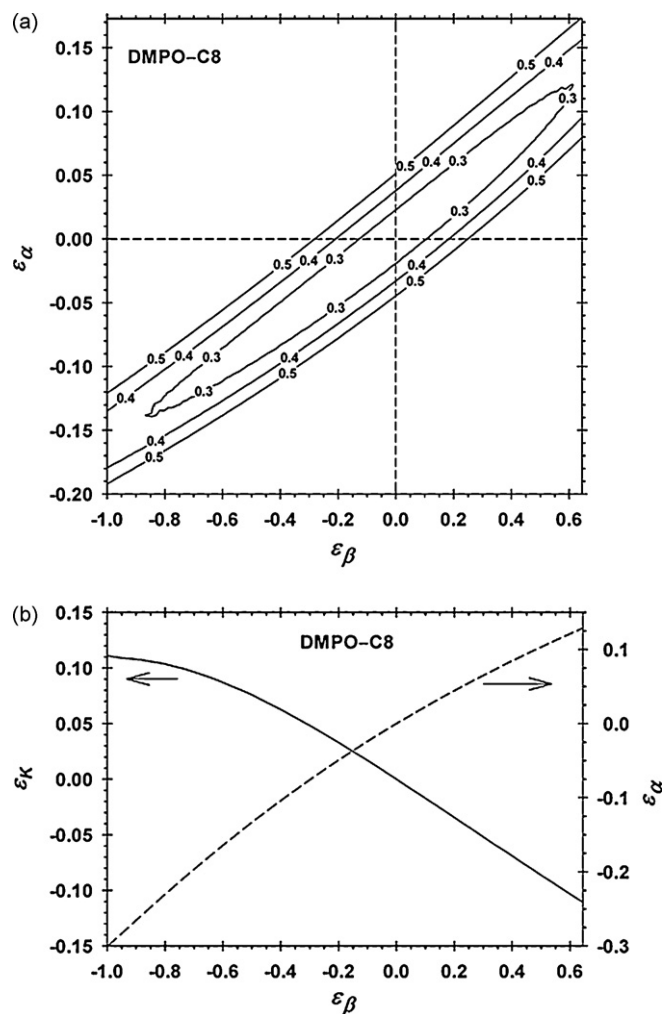
Fig. A.2. Results from processing of experimental data for DMPO–C8 using H–G model: (a) contour plot of the merit function for fixed $K_{s,min}$; (b) change of ε_K and ε_α as a function of ε_β.

Acknowledgement

We are indebted to Miss M. Paraskova for the qualified help in preparing the artwork.

Appendix A. Relative errors of the adjustable parameters

In order to understand the accuracy of the parameters, α_{min}, β_{min}, and $K_{s,min}$, minimizing the merit function, we define their relative errors as follows:

$$\varepsilon_\alpha \equiv \left| \frac{\alpha - \alpha_{min}}{\alpha_{min}} \right|, \quad \varepsilon_\beta \equiv \left| \frac{\beta - \beta_{min}}{\beta_{min}} \right|, \quad \varepsilon_K \equiv \left| \frac{K_s - K_{s,min}}{K_{s,min}} \right| \quad (A.1)$$

We studied the two dimensional contour plot diagrams of the merit function at fixed third parameter. In all cases we found that the relative errors ε_α and ε_K are smaller at fixed value of the interaction parameter, β.

Fig. A.1.a shows the contour plot of the merit function cross-sections at fixed value of $K_{s,min}$ calculated from the experimental data for DMPO–C12 using H–G model. One sees that the minimum is well pronounced and the relative errors of the parameters are of the order of 5%. For deeper understanding of the behavior we fixed the value of β and minimized the merit function with respect to K_s and α. Thus we calculate the functions $K_{s,min}(\beta)$, $\alpha_{min}(\beta)$, and $\chi_{min}(\beta)$. Fig. A.1.b shows the respective relative errors ε_α and ε_K as a function of ε_β for DMPO–C12. In Fig. A.1.b the increase of the calculated merit function from its minimum value is only 0.01 mN/m. The main conclusions are: (i) the area α is calculated with a good precision (error smaller than 4%); (ii) the parameters K_s and β are correlated and their relative errors are of the order of 10%.

When applying the H–G model to the experimental data for DMPO–C8 the conclusions are different. Fig. A.2.a illustrates that the contour 0.3 mN/m covers relative errors of area 10% but the relative errors of the interaction parameter β is from −100% to 60%. Fig. A.2.b has the analogous meaning as Fig. A.1.b but drawn for DMPO–C8. The main conclusions are: (i) the area α and the parameter K_s can be estimated with precision of about 20%; (ii) the interaction parameter β is determined with very large relative error. The same behavior of the merit function was observed for the experimental data for DMPO–C10.

References

[1] N. Nandi, D. Vollhardt, Curr. Opin. Coll. Interface Sci. 13 (2008) 40.
[2] V. Fainerman, D. Vollhardt, J. Phys. Chem. B 113 (2009) 6311.
[3] G. Brezesinski, D. Vollhardt, K. Iimura, H. Colfen, J. Phys. Chem. C 112 (2008) 15777.
[4] V. Fainerman, D. Mobius, R. Miller (Eds.), Surfactant Chemistry, Interfacial Properties, Applications, Elsevier, 2001.
[5] I. Langmuir, J. Am. Chem. Soc. 40 (1918) 1361.
[6] A. Frumkin, Z. Phys. Chem. (Munich) 16 (1925) 466.
[7] M. Volmer, Z. Phys. Chem. 115 (1925) 253.
[8] M. Mulqueen, D. Balnkschtein, Langmuir 16 (2000) 7640.
[9] I.B. Ivanov, K.P. Ananthapadmanabhan, A. Lips, Adv. Colloid Interface Sci. 123–126 (2006) 189.
[10] J.D. Hines, J. Colloid Interface Sci. 180 (1996) 488.
[11] J.N. Israelachvili, Intermolecular and Surface Forces, Academic Press, London, 1992.
[12] L.D. Landau, E.M. Lifshits, Statistical physics, "Naouka", Moscow 1964, in Russian.
[13] T.L. Hill, An Introduction to Statistical Thermodynamics, Addison-Wesley, Reading, MA, 1962.
[14] J. Belton, M. Evans, Trans. Faraday Soc. 41 (1945) 1.
[15] H. Reiss, H. Frisch, J. Lebowitz, J. Chem. Phys. 31 (1959) 369.
[16] E. Helfand, H. Fisch, J. Lebowitz, J. Chem. Phys. 34 (1961) 1037.
[17] C. Tanford, The Hydrophobic Effect. The Formation of Micelles and Biological Membranes, Wiley, New York, 1980.
[18] K. Danov, I.B. Ivanov, K.P. Ananthapadmanabhan, A. Lips, Adv. Colloid Interface Sci. 128–130 (2006) 185.
[19] J. Davies, E. Rideal, Interfacial Phenomena, Academic Press, New York, 1963.
[20] A.I. Russanov, Colloids Surf. A: Physicochem. Eng. Aspects 239 (2004) 105.
[21] R.J. Baxter, J. Chem. Phys. 49 (1968) 2770.
[22] T. Gurkov, I.B. Ivanov, Proceedings of the 4th World Congress on Emulsions, Paper No. 2.1-509, Lyon, France, 2006.
[23] P.C. Hemmer, G. Stell, J. Chem. Phys. 93 (1990) 8220.
[24] T. Kihara, Rev. Modern Phys. 25 (1953) 831.
[25] J. Kirkwood, V. Lewinson, B. Alder, J. Chem. Phys. 20 (1952) 929.
[26] A.V. Makievski, D.O. Grigoriev, Colloids Surf. A: Physicochem. Eng. Aspects 143 (1998) 233.
[27] P. Warszynski, K. Lunkenheimer, J. Phys. Chem. B 103 (1999) 4404.
[28] K. Malysa, R. Miller, K. Lunkenheimer, Colloids Surf. 53 (1991) 47.
[29] K. Lunkenheimer, R. Hirte, J. Phys. Chem. 96 (1992) 8683.
[30] B. Noskov, D. Grigoriev, R. Miller, Langmuir 13 (1997) 295.
[31] R. Viswanathan, J. Garnaes, D.K. Schwartz, J.A.N. Zasadzinski, Proceedings Annual Meeting Microscopy Society of America, 1993.
[32] Handbook of Chemistry, "Himia", Moscow, 1964.